Genetic Ablation of MicroRNA-33 Attenuates Inflammation and Abdominal Aortic Aneurysm Formation via Several Anti-Inflammatory Pathways

Tetsushi Nakao, Takahiro Horie, Osamu Baba, Masataka Nishiga, Tomohiro Nishino, Masayasu Izuhara, Yasuhide Kuwabara, Hitoo Nishi, Shunsuke Usami, Fumiko Nakazeki, Yuya Ide, Satoshi Koyama, Masahiro Kimura, Naoya Sowa, Satoko Ohno, Hiroki Aoki, Koji Hasegawa, Kazuhisa Sakamoto, Kenji Minatoya, Takeshi Kimura, Koh Ono

Objective—Abdominal aortic aneurysm (AAA) is an increasingly prevalent and ultimately fatal disease with no effective pharmacological treatment. Because matrix degradation induced by vascular inflammation is the major pathophysiology of AAA, attenuation of this inflammation may improve its outcome. Previous studies suggested that miR-33 (microRNA-33) inhibition and genetic ablation of miR-33 increased serum high-density lipoprotein cholesterol and attenuated atherosclerosis.

Approach and Results—MiR-33a-5p expression in central zone of human AAA was higher than marginal zone. MiR-33 deletion attenuated AAA formation in both mouse models of angiotensin II– and calcium chloride–induced AAA. Reduced macrophage accumulation and monocyte chemotactic protein-1 expression were observed in calcium chloride–induced AAA walls in miR-33$^{-/-}$ mice. In vitro experiments revealed that peritoneal macrophages from miR-33$^{-/-}$ mice showed reduced matrix metalloproteinase 9 expression levels via c-Jun N-terminal kinase inactivation. Primary aortic vascular smooth muscle cells from miR-33$^{-/-}$ mice showed reduced monocyte chemotactic protein-1 expression by p38 mitogen-activated protein kinase attenuation. Both of the inactivation of c-Jun N-terminal kinase and p38 mitogen-activated protein kinase were possibly because of the increase of ATP-binding cassette transporter A1 that is a well-known target of miR-33. Moreover, high-density lipoprotein cholesterol derived from miR-33$^{-/-}$ mice reduced expression of matrix metalloproteinase 9 in macrophages and monocyte chemotactic protein-1 in vascular smooth muscle cells. Bone marrow transplantation experiments indicated that miR-33–deficient bone marrow cells ameliorated AAA formation in wild-type recipients. MiR-33 deficiency in recipient mice was also shown to contribute the inhibition of AAA formation.

Conclusions—These data strongly suggest that inhibition of miR-33 will be effective as a novel strategy for treating AAA.

Visual Overview—An online visual overview is available for this article. **(*Arterioscler Thromb Vasc Biol*. 2017;37: 2161-2170. DOI: 10.1161/ATVBAHA.117.309768.)**

Key Words: aortic aneurysm, abdominal ■ bone marrow cells ■ inflammation ■ matrix metalloproteinase 9 ■ microRNAs

The prevalence of abdominal aortic aneurysm (AAA) is increasing because of greater longevity and lifestyle changes. It is the third most common cause of cardiovascular death, accounting for 1% to 3% of all deaths in the male population >65 years old.[1] Early diagnosis by computed tomography scanning can be achieved in clinics, but drugs to prevent AAA growth are not available thus far. Because AAA progresses asymptomatically and can result in fatal rupture,[2] developing drug therapy to prevent AAA expansion is an urgent and unmet need. The lack of effective pharmacotherapy for AAA progression is partially because of poor understanding of the mechanisms of AAA occurrence, expansion, and rupture. Epidemiological and pathological studies have provided several clues to the pathophysiology of AAA. Current evidence suggests that inflammation of the aortic wall is a key step in vascular smooth muscle cell (VSMC) apoptosis, endothelial dysfunction, and proteinase activation, which together lead to destruction of the elastic media and fragility of the aortic wall.[3]

Previous drug development has focused on inhibition of extracellular matrix degradation because this process causes aortic wall fragility. However, doxycycline (an inhibitor of

Received on: July 31, 2017; final version accepted on: August 21, 2017.

From the Departments of Cardiovascular Medicine (T.N., T.H., O.B., M.N., T.N., M.I., Y.K., H.N., S.U., F.N., Y.I., S.K., M.K., N.S., T.K., K.O.) and Cardiovascular Surgery (K.S., K.M.), Graduate School of Medicine, Kyoto University, Japan; The Cardiovascular Research Institute, Kurume University, Japan (S.O., H.A.); and Division of Translational Research, National Hospital Organization, Kyoto Medical Center, Japan.

The online-only Data Supplement is available with this article at http://atvb.ahajournals.org/lookup/suppl/doi:10.1161/ATVBAHA.117.309768/-/DC1.

Correspondence to Koh Ono, MD, PhD, Department of Cardiovascular Medicine, Graduate School of Medicine, Kyoto University, 54 Shogoin-kawahara-cho, Sakyo-ku, Kyoto 606-8507, Japan. E-mail kohono@kuhp.kyoto-u.ac.jp

Nonstandard Abbreviations and Acronyms	
AAA	abdominal aortic aneurysm
ABCA1	ATP-binding cassette transporter A1
AMPKα1	AMP-activated protein kinase α1
AngII	angiotensin II
BM	bone marrow
$CaCl_2$	calcium chloride
DKO	double knockout
HDL-C	high-density lipoprotein cholesterol
JNK	c-Jun N-terminal kinase
MAPK	mitogen-activated protein kinase
MCP-1	monocyte chemotactic protein-1
MMP	matrix metalloproteinase
TNFα	tumor necrosis factor α
VSMC	vascular smooth muscle cell

matrix metalloproteinase [MMP], which is one of the major groups of proteinases in AAA pathogenesis) failed to show clear clinical effectiveness against AAA growth,[4] most likely because a wide variety of proteinases are involved in the pathogenesis of AAA.[5] Thus, inhibition of aneurysmal wall inflammation, a process that is upstream of proteinase activation, may be a novel therapeutic target. Several cohort studies and their meta-analyses showed that statins are the most reliable agents among currently available therapeutic options for the prevention of AAA progression and rupture although there are currently no large randomized control trials in progress.[6] Statins are thought to improve AAA prognosis through anti-inflammatory effects resulting from improved cholesterol metabolism and through pleiotropic effects, such as attenuation of protein prenylation.

Recent reports, including ours, have indicated that miR-33 (microRNA-33) regulates cholesterol metabolism by targeting ATP-binding cassette transporter A1 (ABCA1), thus reducing high-density lipoprotein cholesterol (HDL-C) levels, and miR-33 deficiency ameliorates atherosclerosis in mice.[7–11] MiRs are a well-defined species of noncoding RNAs, and evidence is accumulating that this class of genes plays crucial roles in many physiological and pathological processes. Indeed, several miRs affecting AAA have been reported; their targets include proteinases, extracellular matrix production, vascular cell homeostasis, and inflammation.[12] However, although clinical evidence also suggests that serum cholesterol level,[13] cholesterol efflux,[14] and ABCA1 polymorphism[15] are associated with AAA prevalence, there are no reports of miRs associated with cholesterol homeostasis and AAA. Here, we speculated that loss of miR-33 may exert a beneficial role on AAA formation in addition to having atheroprotective effects because anti–miR-33 treatments have anti-inflammatory properties[10] that are also observed in statin treatment. Indeed, circulating miR-33a-5p is reported to be elevated in patients with AAA compared with healthy controls.[16]

In the present study, we found elevated miR-33 expression in central zones compared with in marginal zones in human AAA. As an interventional study, we investigated the effect of miR-33 deficiency in a mouse model of angiotensin II (AngII)–induced AAA, and then confirmed the effect of this deficiency on inflammation in a calcium chloride ($CaCl_2$)–induced AAA model. In vitro experiments revealed that miR-33 deficiency reduced MMP9 expression levels in macrophages and MCP-1 (monocyte chemotactic protein-1) levels in VSMCs and augmented the anti-inflammatory effects of HDL-C. Finally, we performed bone marrow (BM) transplantation experiments using miR-33–deficient mice and showed that miR-33 deficiency in BM cells and other recipient cells had a distinct beneficial effect on AAA formation. These data strongly suggest that inhibition of miR-33 is a promising strategy for treating AAA.

Materials and Methods

Materials and Methods are available in the online-only Data Supplement.

Results

MiR-33 Deletion Attenuates AAA Both in AngII and $CaCl_2$ Models

We compared the expression levels of miR-33 between the central and marginal zones of human AAA. Although miR-33b-5p expression levels were not different, miR-33a-5p levels were elevated in the central zone compared with in the marginal zone in all samples analyzed (Figure I in the online-only Data Supplement).

As interventional analyses, we conducted in vivo experiments using previously generated C57BL/6 background miR-$33^{-/-}$ mice.[9] While humans have 2 homologues of miR-33 (a and b), rodents have only 1 miR-33 locus, which is equivalent to miR-33a. We developed a mouse model of AAA by continuous subcutaneous infusion of AngII for 4 weeks to Western-type diet–fed C57BL/6 background *Apoe*$^{-/-}$ mice (Figure IIA in the online-only Data Supplement)[17] and compared the formation of AAA between miR-$33^{+/+}$ *Apoe*$^{-/-}$ (single knockout) and miR-$33^{-/-}$ *Apoe*$^{-/-}$ (double knockout [DKO]) mice. Successful AngII delivery was confirmed by optimally raised blood pressure (Figure IIB in the online-only Data Supplement). Body weight, blood pressure, and heart rate were not significantly different between single knockout and DKO mice (Figure IIB–IID in the online-only Data Supplement). The baseline morphology and diameter of aortas in vehicle-treated mice were not different between groups (Figure 1A and 1B). AAA was successfully induced, dissecting media, and generating pseudolumen, as reported previously[18] (Figure IIE in the online-only Data Supplement). The expression of miR-33 was elevated in AngII-treated suprarenal abdominal aortas (Figure IIF in the online-only Data Supplement). The AAA diameter in DKO mice was significantly smaller than in single knockout mice (Figure 1A–1C), and AAA in DKO mice was less severe (Figure 1D), as determined using a previously reported severity scale for AAA[19] (briefly detailed in the Materials and Methods in the online-only Data Supplement). Moreover, whereas 40% of single knockout mice died from aortic dissection and rupture within 1 week after the initiation of continuous infusion of AngII, as reported previously,[20] significantly fewer (30.77%) DKO mice died within this period (Figure 1E).

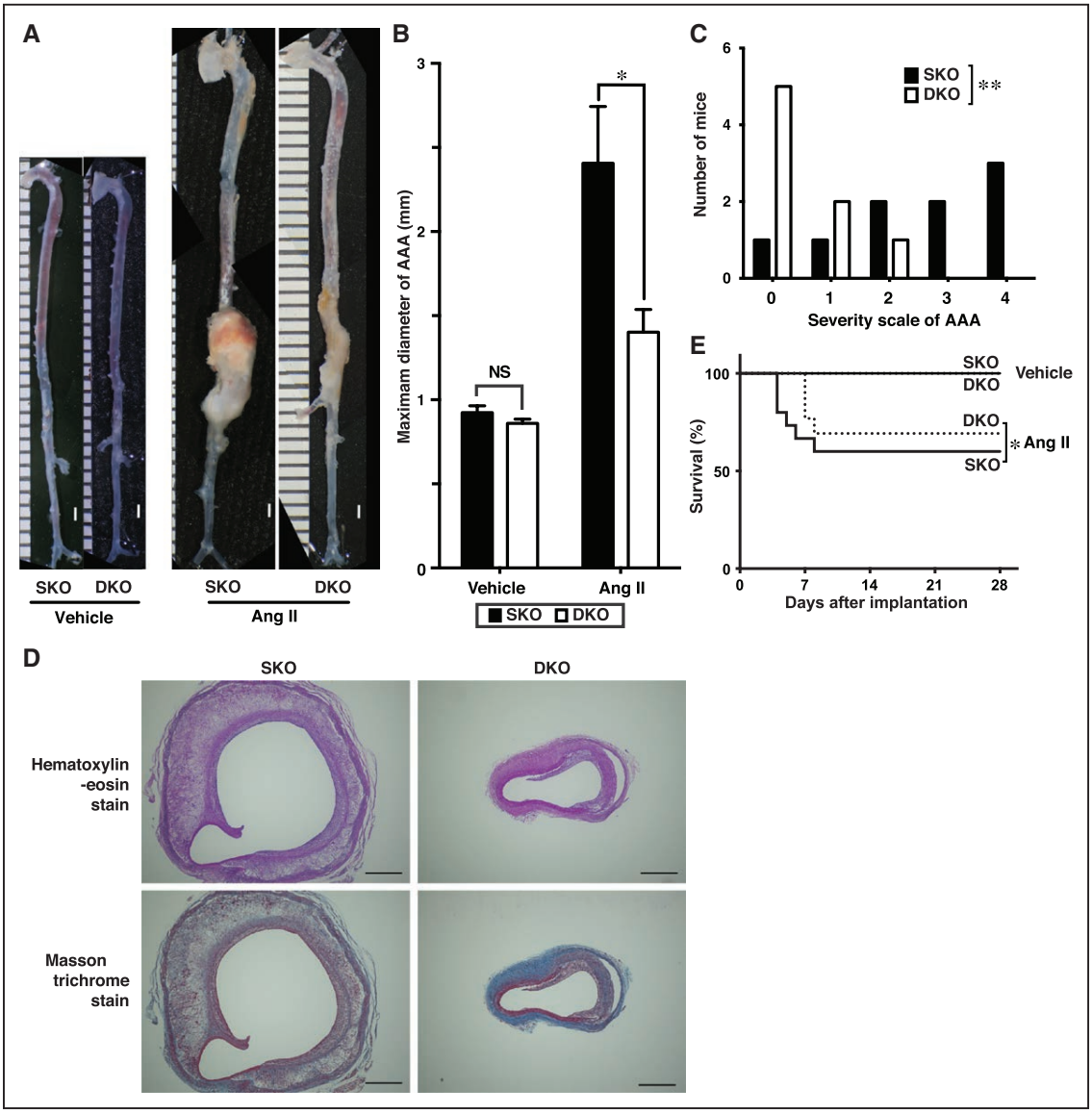

Figure 1. A, Representative photographs of sham and angiotensin (Ang) II–induced abdominal aortic aneurysm (AAA), including measures on the left side. White bars represent 1 mm. **B**, Graph of maximum diameter of sham and AngII-induced AAA. n=11 to 12 mice in the sham group, and n=9 mice in the AngII group. Data are presented as mean±SEMs. *P<0.05 calculated using the Mann–Whitney test. **C**, Representative immunohistochemistry of AAA (most dilated part) from AngII-treated single knockout (SKO) and double knockout (DKO) mice. Black bars indicate 500 μm. **D**, Severity of AngII-induced AAAs in SKO and DKO mice was scored from type 0 to 4 pathology based on the commonly used severity classification scheme described previously.[19] **P<0.01 calculated using χ^2 for trend. **E**, Survival of sham and AngII-induced AAA model. *P<0.05 calculated using log-rank test, n=11 to 12 mice in the sham group and n=9 mice in the AngII group. Mice that died because of rupture were not included in the analyses in (**B**) and (**D**). NS indicates not significant.

Next, we used another model in which AAA was induced by infrarenal periaortic application of $CaCl_2$.[21] AAA was successfully induced compared with sham-operated mice (Figure 2A and 2B). The baseline morphology and diameter of aortas in sham-operated mice were not different between groups (Figure 2A–2C). The mean maximum diameter of $CaCl_2$-induced AAA was significantly smaller in miR-33$^{-/-}$ mice compared with miR-33$^{+/+}$ mice (Figure 2A and 2B). In addition, elongation of the infrarenal aorta was attenuated more in miR-33$^{-/-}$ mice than in miR-33$^{+/+}$ mice (Figure 2C). Elastica van Gieson staining revealed fragmentation of the elastic layers of $CaCl_2$-treated aorta compared with sham controls in miR-33$^{+/+}$ mice (Figure IIIA in the online-only Data Supplement). MiR-33 expression in the AAA wall was increased 1 week after $CaCl_2$ application and decreased gradually afterward (Figure IIIB in the online-only Data Supplement). There were no significant differences between miR-33$^{+/+}$ and miR-33$^{-/-}$ mice in baseline characteristics, such as body weight, blood pressure, or heart rate (Figure IIIC–IIIE in the online-only Data Supplement). Although serum HDL level was reported to be elevated in miR-33$^{-/-}$ mice,[9] serum HDL levels in and miR-33$^{+/+}$ and miR-33$^{-/-}$ mice 7 days after $CaCl_2$ application were 50.7±3.91 and 54.2±1.81 mg/dL, respectively (n=8 and 9).

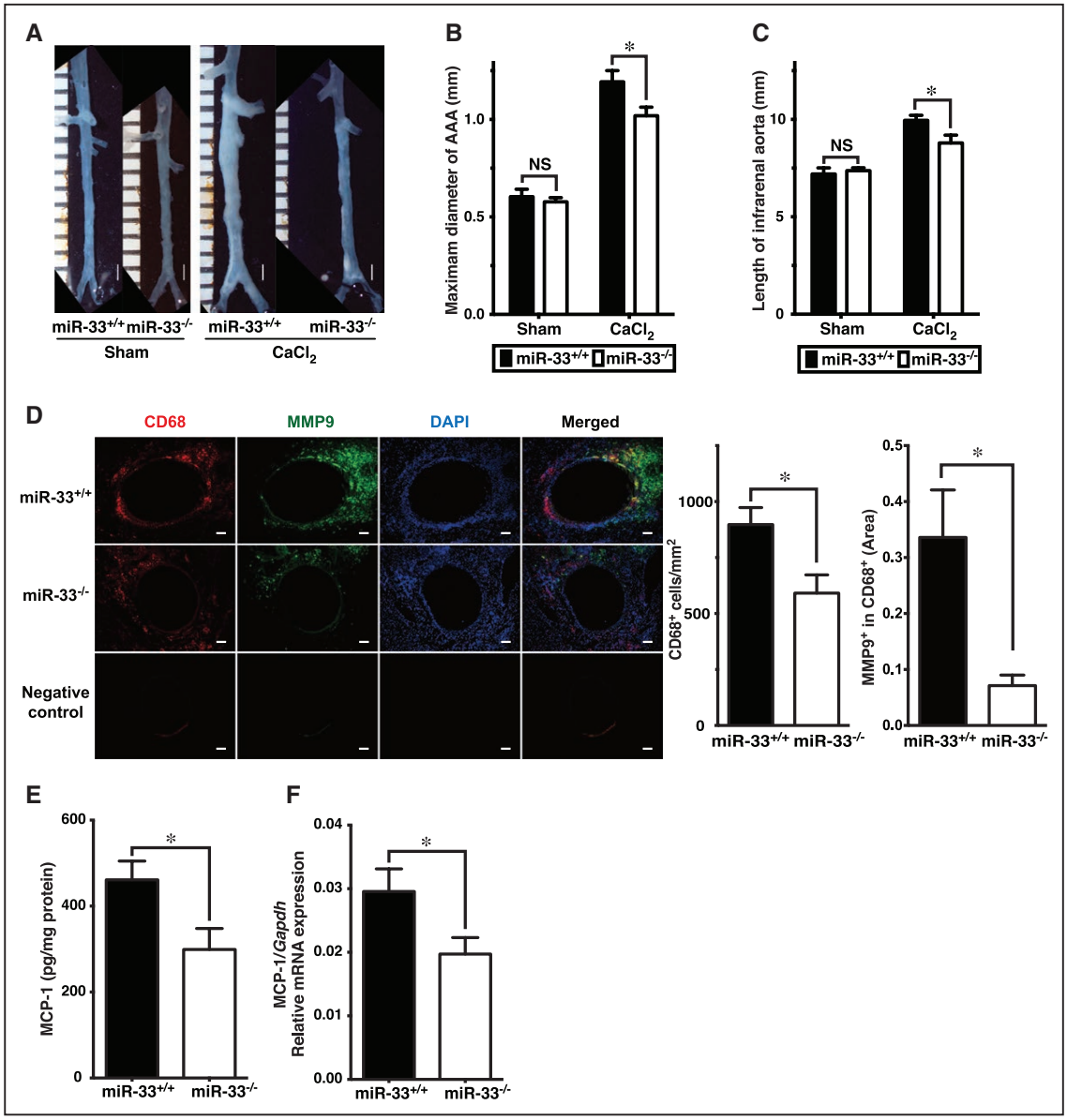

Figure 2. Genetic deletion of microRNA (miR-33) attenuates calcium chloride ($CaCl_2$)–induced abdominal aortic aneurysm (AAA). **A**, Representative photographs of sham and $CaCl_2$-induced AAA in miR-33$^{+/+}$ and miR-33$^{-/-}$ mice. White bars indicate 1 mm. **B**, Graph of maximum diameter of sham and $CaCl_2$-induced AAA, n=7 mice in the sham group and n=14 to 15 mice in the $CaCl_2$ group. Mann–Whitney test. **C**, Graph of length of abdominal aorta between left renal artery and bifurcation of sham and $CaCl_2$-induced AAA, n=6 in the sham group and n=12 to 14 in the $CaCl_2$ group. Mann–Whitney test. **D**, CD68-positive cells were counted, and matrix metalloproteinase (MMP) 9–positive area in the CD68-positive area was measured in sections of $CaCl_2$-induced AAA wall at 1 wk after treatment. Student *t* test, n=14 to 15. White bars indicate 100 μm. **E** and **F**, Monocyte chemotactic protein (MCP)-1 expression levels in AAA walls were assessed using an enzyme-linked immunosorbent assay (**E**), and quantitative real-time polymerase chain reaction (**F**). Student *t* test, n=10. **P*<0.05. All data represent means±SEM. NS indicates not significant.

Macrophage Infiltration and MMP9 and MCP-1 Expression Levels Are Reduced in $CaCl_2$-Induced AAA Walls of MiR-33$^{-/-}$ Mice

To determine the mechanisms underlying the attenuation of AAA in miR-33$^{-/-}$ mice, we analyzed AAA walls at 7 days after the application of $CaCl_2$. In this and subsequent experiments, we used the $CaCl_2$ model, in which AAA is induced purely by vascular inflammation rather than plaque formation, although the $CaCl_2$-induced AAA model does not induce rupture or death.[22]

Accumulation of CD68$^+$ macrophages in AAA walls was assessed as a marker of inflammation in the AAA wall. Macrophage infiltration was reduced in miR-33$^{-/-}$ mice compared with miR-33$^{+/+}$ mice (Figure 2D). Total gelatinase activity of MMPs, which play a central role in AAA pathophysiology by degrading the extracellular matrix, as assessed by in situ zymography, was also attenuated in miR-33$^{-/-}$ mice (Figure IIIF in the online-only Data Supplement). This was replicated in the AngII model (Figure IIIG in the online-only Data Supplement).

Moreover, the MMP9-positive area in the CD68-positive area was significantly reduced in miR-33$^{-/-}$ mice compared with miR-33$^{+/+}$ mice (Figure 2D).

It is known that monocytes originating from BM extravasate into vessel walls by chemoattractant-receptor interaction and subsequently differentiate into macrophages. Therefore, given that MCP-1 is a major chemoattractant of monocytes/macrophages, we measured its expression level in the AAA wall. MCP-1 expression was significantly reduced in miR-33$^{-/-}$ mice both in enzyme-linked immunosorbent assay and quantitative real-time polymerase chain reaction analyses (Figure 2E and 2F). Immunohistochemistry of MCP-1 also performed for baseline and AngII model (Figure IVA and IVB in the online-only Data Supplement).

$CaCl_2$-treated miR-33$^{-/-}$ and miR-33$^{+/+}$ mice did not show a significant difference in the proportion of the inflammatory Ly-6c^{high} subset of monocytes in blood (Figure V in the online-only Data Supplement).

Macrophages in MiR-33$^{-/-}$ Mice Exhibit Reduced M1/M2 Marker Expression and MMP9 Activity

MMPs and MCP-1 are mainly released from macrophages or VSMCs in inflammatory vascular walls.[23] Therefore, we examined the phenotypes of macrophages and VSMCs from miR-33$^{-/-}$ mice in vitro.

Quantitative real-time polymerase chain reaction analysis revealed decreased M1/M2 marker ratios in miR-33$^{-/-}$ peritoneal macrophages as consistent with previous report[10] (Figure 3A). In particular, *Mmp9*, which is a M1 marker, was significantly decreased in these cells. MMP9 activity in the conditioned medium of miR-33$^{-/-}$ macrophages, as assessed by gelatin zymography, was also significantly reduced (Figure 3B). Finally, *MMP9* expression was reduced in miR-33 knocked-down THP-1 macrophages (Figure VIA in the online-only Data Supplement).

Tumor necrosis factor α (TNFα) is thought to be one of the central cytokines in AAA progression, and it acts by inducing the release of proteases that degrade the extracellular matrix.[24] Thus, we analyzed *Mmp9* expression in macrophages stimulated by TNFα and found attenuated *Mmp9* expression in miR-33$^{-/-}$ macrophages (Figure 3C).

MiR-33 was reported to increase the M1/M2 marker ratio in macrophages directly targeting AMP-activated protein kinase α1 (AMPKα1).[10] AMPKα1 expression in miR-33$^{-/-}$ peritoneal macrophages was consistently increased (Figure 3D), and miR-33 overexpression in THP-1 macrophages suppressed AMPKα1 expression (Figure VIB in the online-only Data Supplement). However, AMPKα1 knockdown did not attenuate the difference in *Mmp9* expression between miR-33$^{+/+}$ and miR-33$^{-/-}$ macrophages (Figure 3E). Although ABCA1, which is one of the well-known miR-33 targets, was indeed elevated in miR-33$^{-/-}$ macrophages (Figure VIC in the online-only Data Supplement) as reported previously.[9] To investigate whether ABCA1 is involved in the *Mmp9* expression in macrophages, we performed siRNA-mediated knockdown of ABCA1. Both miR-33$^{+/+}$ and miR-33$^{-/-}$ macrophages showed similar levels in *Mmp9* in the condition of siRNA-mediated knockdown of ABCA1 (Figure 3F).

However, it was reported that c-Jun N-terminal kinase (JNK), one of inflammatory mitogen-activated protein kinase (MAPK), upregulated MMP9, and JNK inhibition caused the regression of AAA formation.[24] Therefore, we analyzed JNK activity in macrophages with or without TNFα stimulation. Western blotting analysis of macrophages revealed significantly reduced JNK activity in miR-33$^{-/-}$ macrophages after TNFα stimulation (Figure 3G). In contrast, p38 MAPK, the other inflammatory MAPK, was unchanged between the groups (Figure VID in the online-only Data Supplement). Moreover, JNK inhibition by SP600125 canceled the effect of miR-33 deletion on *Mmp9* expression in peritoneal macrophages (Figure 3H). It is known that ABCA1 knockout activate JNK pathway.[25] Thus, MMP9 downregulation in miR-33$^{-/-}$ macrophages was suspected to be mediated by reduced JNK activity through the increase of ABCA1 levels.

Although macrophages are thought to be another source of MCP-1, there was no difference in the concentration of MCP-1 in macrophage-conditioned medium between the 2 groups (Figure VIE in the online-only Data Supplement).

Deletion of MiR-33 Attenuates MCP-1 Expression in VSMCs

In immunohistochemical analysis in mouse aortas, MCP-1 was colocalized with α smooth muscle actin (Figure IVA in the online-only Data Supplement), indicating that the major source of MCP-1 was VSMCs in this setting. Therefore, we measured the expression of MCP-1 in primary aortic VSMCs derived from miR-33$^{+/+}$ and miR-33$^{-/-}$ mice. MCP-1 mRNA expression assessed by quantitative real-time polymerase chain reaction was significantly decreased in VSMCs from miR-33$^{-/-}$ mice compared with those from miR-33$^{+/+}$ mice (Figure 4A). MCP-1 protein levels quantified by enzyme-linked immunosorbent assay in the conditioned medium were also significantly reduced in VSMCs from miR-33$^{-/-}$ mice compared with the controls (Figure 4B). MiR-33 knockdown in human VSMCs consistently downregulated MCP-1 expression (Figure VIIA in the online-only Data Supplement).

$CaCl_2$-induced AAA walls (Figure VIIB in the online-only Data Supplement) and mouse primary VSMCs (Figure 4C) from miR-33$^{-/-}$ mice showed increased levels of ABCA1. This was consistent with miR-33–overexpressing rat VSMCs (Figure VIIC in the online-only Data Supplement). Because ABCA1 is a major target of miR-33 that affects inflammation via lipid rafts,[9,25] we hypothesized that reduced MCP-1 expression in miR-33$^{-/-}$ VSMCs is a consequence of elevated ABCA1 expression. Knockdown of ABCA1 in primary mouse VSMCs eliminated the difference in MCP-1 expression levels between wild-type and miR-33$^{-/-}$ mice (Figure 4D).

It is known that p38 MAPK is crucial for the regulation of MCP-1.[26,27] Thus, we examined p38 MAPK activity in miR-33$^{-/-}$ VSMCs after TNFα stimulation and found that its activity was significantly lower than that in miR-33$^{+/+}$ VSMCs (Figure 4E). In contrast, p38 MAPK activity was elevated in miR-33–overexpressing rat VSMCs (Figure VIID in the online-only Data Supplement). When VSMCs were

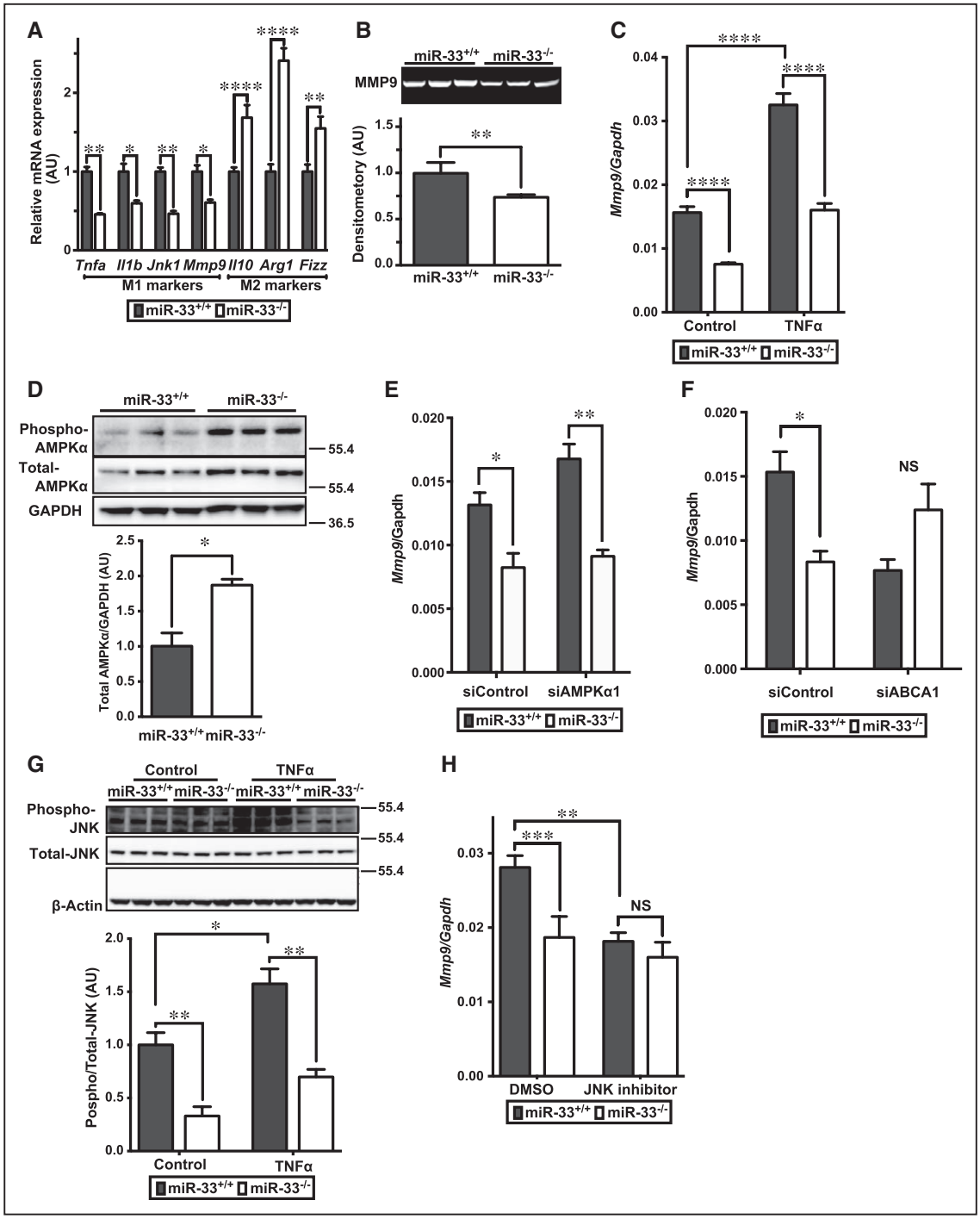

Figure 3. A, Quantitative real-time polymerase chain reaction (qRT-PCR) analysis of M1/M2 markers in peritoneal macrophages. Two-way ANOVA with Bonferroni multiple comparison test, n=3. **B**, Conditioned medium from peritoneal macrophages was assessed by gelatin zymography. Mann–Whitney test, n=6. **C**, Peritoneal macrophages were stimulated with 25 ng/mL tissue necrosis factor (TNF) α for 3 h and assessed by qRT-PCR. Two-way ANOVA with Tukey multiple comparison test, n=6. **D**, Western blotting analysis in peritoneal macrophages, stimulated with 25 ng/mL TNFα for 15 min. Two-way ANOVA with Tukey multiple comparison test, n=3 per group. **E**, Peritoneal macrophages were transfected by siAMPKα1 or control and assessed by qRT-PCR. Two-way ANOVA with Tukey multiple comparison test, n=3. **F**, Peritoneal macrophages were transfected by siABCA1 and control. Two-way ANOVA with Tukey multiple comparison test, n=3. **G**, Peritoneal macrophages were assessed by Western blotting. Two-way ANOVA with Tukey multiple comparison test, n=3. **H**, Peritoneal macrophages were stimulated with 25 ng/mL TNFα for 3 h and with 100 μmol/L of SP600125 (c-Jun N-terminal kinase [JNK] inhibitor) or dimethyl sulfoxide (DMSO) as vehicle. Two-way ANOVA with Tukey multiple comparison test, n=4 to 6. All data represent means±SEM. **P*<0.05, ***P*<0.01, ****P*<0.001, *****P*<0.0001. These are representatives of ≥3 biological replicates. ABCA1 indicates ATP-binding cassette transporter A1; AMPK, AMP-activated protein kinase α1; AU, arbitrary unit; miR, microRNA; MMP, matrix metalloproteinase; and NS, not significant.

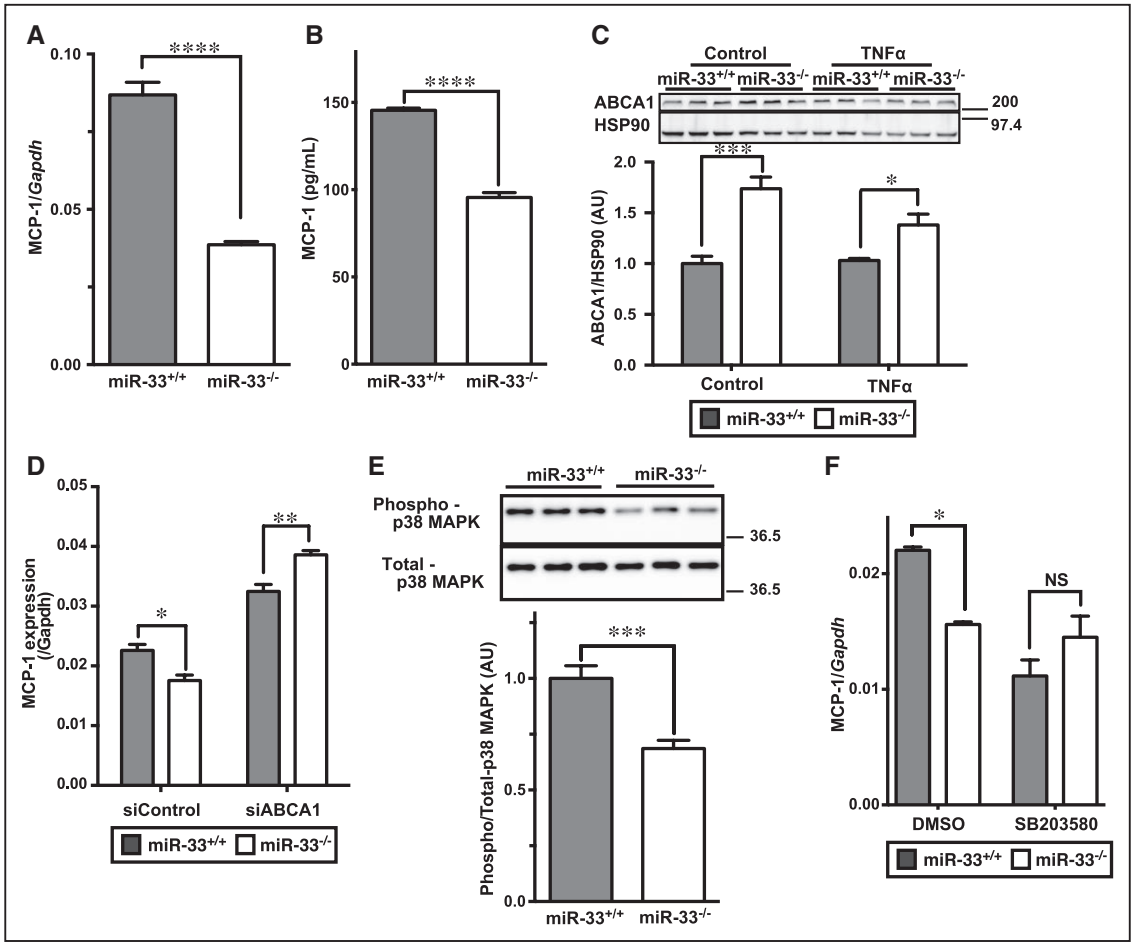

Figure 4. A and **B**, Quantitative real-time polymerase chain reaction (qRT-PCR) using cell lysates (**A**) and enzyme-linked immunosorbent assay using conditioned medium (**B**) of MCP-1 (monocyte chemotactic protein-1) in primary aortic vascular smooth muscle cells (VSMCs). Student *t* test, n=6. **C**, ATP-binding cassette transporter A1 (ABCA1) was assessed by Western blotting in VSMCs with or without 15 min of stimulation with 100 ng/mL tissue necrosis factor (TNF) α. Two-way ANOVA with Tukey multiple comparison test, n=3. **D**, Mouse primary VSMCs were transfected by siRNA for ABCA1 and control and assessed by qRT-PCR. Two-way ANOVA with Tukey multiple comparison test, n=3. **E**, VSMCs were stimulated with TNFα for 15 min and analyzed by Western blotting. Student *t* test, n=6. **F**, Primary aortic VSMCs were incubated with 20 μmol/L SB203580 or dimethyl sulfoxide (DMSO) as vehicle for 1.5 h and analyzed by qRT-PCR. Two-way ANOVA with Tukey multiple comparison test, n=3. This result is representative of 3 biological replicates. All data represent means±SEM. **P*<0.05, ***P*<0.01, ****P*<0.001, *****P*<0.0001. AU indicates arbitrary unit; HSP90, heat shock protein 90; MAPK, mitogen-activated protein kinase; and miR, microRNA.

incubated with a p38 MAPK-specific inhibitor (SB203580; 20 μmol/L) or dimethylsulfoxide (vehicle), the difference in MCP-1 mRNA expression between miR-33$^{+/+}$ and miR-33$^{-/-}$ VSMCs was abolished (Figure 4F). Taken together, MCP-1 reduction in miR-33$^{-/-}$ VSMCs was thought to be mediated by upregulation of ABCA1 and attenuation of p38 MAPK activity.

The activity of JNK did not differ between miR-33$^{+/+}$ and miR-33$^{-/-}$ VSMCs (Figure VIIE in the online-only Data Supplement).

HDL-C in MiR-33$^{-/-}$ Mice Has Augmented Anti-Inflammatory Properties in Macrophages and VSMCs

Whereas HDL-C levels were reported to increase with miR-33 inhibition[7,11] and miR-33 deficiency,[9] the anti-inflammatory effects of HDL-C,[28] such as MMP9 reduction in macrophages[29] and MCP-1 reduction in VSMCs,[30] are well-known. Therefore, we examined the effect of HDL-C on TNFα-induced MMP9 expression in macrophages. Compared with controls, human-derived HDL-C at 0.1 or 0.5 mg/mL reduced *Mmp9* expression in peritoneal macrophages in a dose-dependent manner (Figure 5A). Next, we compared the effect of HDL-C against *Mmp9* expression in macrophages using HDL-C derived from miR-33$^{+/+}$ (wild-type HDL) and miR-33$^{-/-}$ (knockout HDL) mice. Knockout HDL mice showed more beneficial effects against TNFα-induced *Mmp9* expression in macrophages than wild-type HDL (Figure 5B). Moreover, HDL-C reduced MCP-1 expression in rat VSMCs in a dose-dependent manner (Figure 5C), and this effect was much more prominent in knockout HDL compared with wild-type HDL mice (Figure 5D). Taken together, these results indicated that wild-type HDL exhibited more potent anti-inflammatory effects than knockout HDL.

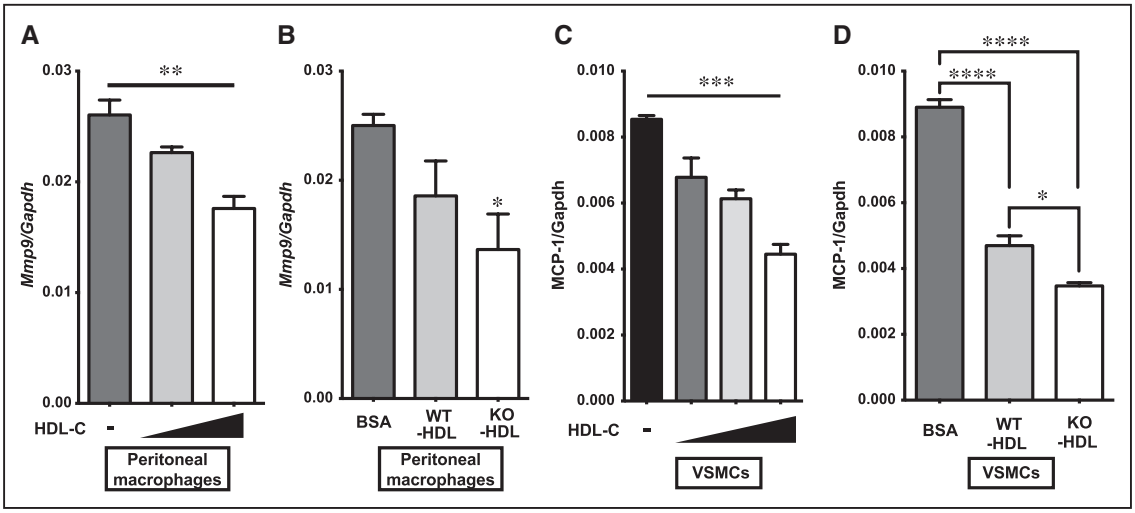

Figure 5. A, Peritoneal macrophages derived from C57BL/6J mice were pre-incubated with or without human high-density lipoprotein cholesterol (HDL-C; 0.1 or 0.5 mg/mL) for 4.5 h and subsequently stimulated with tissue necrosis factor (TNF) α (25 ng/mL) for 3 h. One-way ANOVA with post-test for linear trend, n=3. **B**, Peritoneal macrophages were pre-incubated with 0.2% of bovine serum albumin (BSA) as control or HDL-C collected from miR-33 (microRNA-33)$^{+/+}$ (wild-type [WT]-HDL) or miR-33$^{-/-}$ (knockout [KO]-HDL) mice and subsequently stimulated with TNFα for 3 h. Non-parametric 1-way ANOVA with post-test using Dunn multiple comparisons test, n=3. **C**, Rat vascular smooth muscle cells (VSMCs) were incubated with 0, 1, 3, or 10 μg/mL human HDL-C for 12 h, and monocyte chemotactic protein-1 (MCP-1) expressions were assessed by quantitative real-time polymerase chain reaction. One-way ANOVA with post-test for linear trend, n=3. **D**, Rat VSMCs were incubated with 0.5% BSA or 5% WT-HDL or KO-HDL for 3 h. One-way ANOVA with Tukey multiple comparisons test, n=3. All experiments are representatives of ≥3 biological replicates. All data represent means±SEM. **P*<0.05, ***P*<0.01, ****P*<0.001, *****P*<0.0001.

BM Transplantation Exhibits Both Donor and Recipient Effects of MiR-33 Deletion in a $CaCl_2$-Induced AAA Model

In vitro experiments suggested that macrophages, VSMCs, and HDL-C from miR-33$^{-/-}$ mice have distinct beneficial effects on AAA formation. To distinguish and clarify the effects of each component on AAA formation in vivo, we conducted BM transplantation experiments in both miR-33$^{+/+}$ and miR-33$^{-/-}$ mice. Six weeks after BM transplantation, the recipient mice were treated with $CaCl_2$ to induce AAA formation (Figure 6A). Transplantation of miR-33$^{-/-}$ BM cells into miR-33$^{+/+}$ mice significantly inhibited aneurysm formation (Figure 6B and 6C; Figure VIII in the online-only Data Supplement). In addition, miR-33$^{-/-}$ recipient mice transplanted with either miR-33$^{+/+}$ or miR-33$^{-/-}$ BM cells demonstrated decreased AAA diameter compared with miR-33$^{+/+}$ recipient mice transplanted with miR-33$^{+/+}$ BM cells (Figure 6B and 6C; Figure VIII in the online-only Data Supplement). HDL-C levels were significantly increased in miR-33$^{-/-}$ recipient mice compared with miR-33$^{+/+}$ recipient mice (Figure 6D). Thus, the difference in HDL-C levels was thought to be a recipient effect of AAA attenuation in miR-33$^{-/-}$ mice. These results suggested that both recipient effects (HDL-C and VSMCs) and donor effect (macrophages) contributed considerably to the reduction of AAA formation in miR-33$^{-/-}$ mice.

Discussion

We used 2 distinct mouse AAA models and in vitro experiments to demonstrate that genetic deletion of miR-33 suppressed AAA formation by several different mechanisms: serum HDL-C elevation, as well as MMP9 reduction in macrophages and MCP-1 reduction in VSMCs, through suppression of JNK and p38 MAPK activity, respectively. We also analyzed the contribution of previously known miR-33 target genes. AMPKα1 was shown to be upregulated by the inhibition of miR-33 and suppress the inflammatory phenotypes in macrophages.[13] However, there was no effect of AMPKα1 knockdown on the difference in *Mmp9* expression between miR-33$^{+/+}$ and miR-33$^{-/-}$ macrophages. However, ABCA1 knockdown abolished the difference in *Mmp9* expression between these macrophages. Moreover, knockdown of ABCA1 in primary mouse VSMCs eliminated the difference in MCP-1 expression levels between wild-type and miR-33$^{-/-}$ mice (Graphical Abstract).

In both models, miR-33 deletion attenuated AAA formation. Macrophage infiltration and MMP9 expression in macrophages were attenuated in miR-33$^{-/-}$ AAA walls. MCP-1, the major chemoattractant of monocytes/macrophages, was also decreased in miR-33$^{-/-}$ mice. These results were consistent with previous study that reported miR-33–mediated M1/M2 marker elevation and reduction of serum MCP-1 levels in anti-miR-33–treated mice.[10]

Serum HDL-C levels in BM-transplanted miR-33$^{-/-}$ mice revealed that the main contributor of serum HDL-C elevation in miR-33$^{-/-}$ mice was not deletion of miR-33 in BM cells. This result was consistent with a previous report in *Abca1*$^{-/-}$ mice,[31] which revealed that reduced serum HDL-C levels in *Abca1*$^{-/-}$ mice were because of a lack of ABCA1 in the liver and not to BM cells. These results suggested that serum HDL-C elevation in miR-33$^{-/-}$ mice was caused mainly by hepatic ABCA1 elevation. In relation to AAA, serum HDL-C or apolipoprotein A1 levels were reported to negatively correlate with AAA prevalence and progression, and the effect of HDL-C on AAA was thought to be much stronger than its

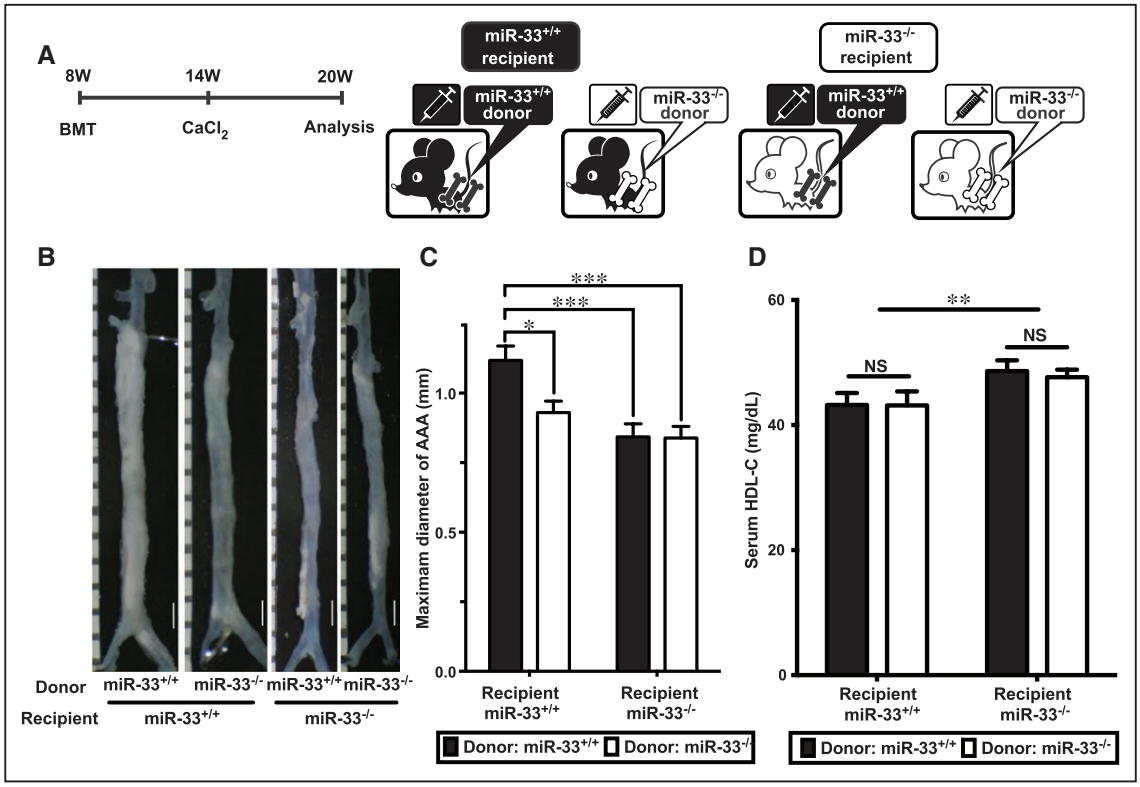

Figure 6. Scheme (**A**), representative photographs (**B**), graphed maximum diameter (**C**), serum high-density lipoprotein cholesterol (**D**) of calcium chloride ($CaCl_2$)–induced abdominal aortic aneurysm (AAA) in bone marrow transplantation (BMT) experiments. White bars indicate 1 mm. Two-way ANOVA with Tukey multiple comparison test, n=15 to 20. *P<0.05, **P<0.01, ***P<0.001. All data represent means±SEM. HDL-C indicates high-density lipoprotein cholesterol; miR-33, microRNA-33; and NS, not significant.

effect on preventing plaque formation because inflammatory mechanisms are more important for AAA. Furthermore, the ABCA1/HDL interaction itself is thought to have distinct anti-inflammatory effects.[32]

As mentioned in the first paragraph, statins were reported to be the most reliable agents for preventing AAA progression and rupture,[6] and several supportive basic research studies indicated that the mechanisms underlying this effect were anti-inflammation resulting from improved cholesterol metabolism and distinct pleiotropic effects, such as attenuation of protein isoprenylation.[33,34] Taken together with speculation on the anti-AAA effects of statins, AAA may be effectively prevented by anti-inflammation and improved cholesterol metabolism, the latter because of either statins or anti–miR-33. MiRs can be suppressed by antisense oligonucleotides, some of which, including anti–miR-33, are currently being investigated in clinical or preclinical trials.[35,36] In contrast, statins are also known to increase miR-33 and decrease ABCA1 expression.[37] Thus, miR-33 inhibition by an antisense oligonucleotide in combination with statins may enhance the anti-AAA effect of statins. At the same time, these results suggested that the combination of improving cholesterol metabolism and achieving distinct anti-inflammation should be targeted for developing more effective strategies to improve AAA prognosis, whereas many pathways are said to affect AAA.

In summary, miR-33 deletion ameliorated AAA formation in $CaCl_2$- and AngII-induced AAA models, and an in vitro study and BM transplantation experiments showed that attenuated expression of MMP9 in macrophages as a donor effect and elevated HDL-C levels and reduced MCP-1 expression in VSMCs as recipient effects are all thought to contribute to the reduction of AAA in miR-33$^{-/-}$ mice. A novel miR-33/cholesterol axis in AAA pathogenesis was uncovered in this study, and these results strongly suggest that inhibition of miR-33 may be a novel therapeutic strategy for AAA.

Sources of Funding

This work was supported by grants from the Ministry of Education, Culture, Sports, Science, and Technology (MEXT) and Japan Society for the Promotion of Science KAKENHI grant numbers 26116716, 26293186, and 25670383 to K. Ono, 26860556 to Y. Kuwabara, 20565577 to T. Horie, and 25293182 to T. Kimura.

Disclosures

None.

References

1. Sakalihasan N, Limet R, Defawe OD. Abdominal aortic aneurysm. *Lancet*. 2005;365:1577–1589. doi: 10.1016/S0140-6736(05)66459-8.
2. Powell JT, Greenhalgh RM. Clinical practice. Small abdominal aortic aneurysms. *N Engl J Med*. 2003;348:1895–1901. doi: 10.1056/NEJMcp012641.
3. Peshkova IO, Schaefer G, Koltsova EK. Atherosclerosis and aortic aneurysm—is inflammation a common denominator? *FEBS J*. 2016;283:1636–1652. doi: 10.1111/febs.13634.
4. Meijer CA, Stijnen T, Wasser MN, Hamming JF, van Bockel JH, Lindeman JH; Pharmaceutical Aneurysm Stabilisation Trial Study Group. Doxycycline for stabilization of abdominal aortic aneurysms: a randomized trial. *Ann Intern Med*. 2013;159:815–823. doi: 10.7326/0003-4819-159-12-201312170-00007.

5. Ailawadi G, Eliason JL, Upchurch GR Jr. Current concepts in the pathogenesis of abdominal aortic aneurysm. *J Vasc Surg*. 2003;38:584–588.
6. Gokani VJ, Sidloff D, Bath MF, Bown MJ, Sayers RD, Choke E. A retrospective study: factors associated with the risk of abdominal aortic aneurysm rupture. *Vascul Pharmacol*. 2015;65–66:13–16. doi:10.1016/j.vph.2014.11.006.
7. Rayner KJ, Sheedy FJ, Esau CC, Hussain FN, Temel RE, Parathath S, van Gils JM, Rayner AJ, Chang AN, Suarez Y, Fernandez-Hernando C, Fisher EA, Moore KJ. Antagonism of miR-33 in mice promotes reverse cholesterol transport and regression of atherosclerosis. *J Clin Invest*. 2011;121:2921–2931. doi: 10.1172/JCI57275.
8. Horie T, Baba O, Kuwabara Y, et al. MicroRNA-33 deficiency reduces the progression of atherosclerotic plaque in ApoE-/- mice. *J Am Heart Assoc*. 2012;1:e003376. doi: 10.1161/JAHA.112.003376.
9. Horie T, Ono K, Horiguchi M, Nishi H, Nakamura T, Nagao K, Kinoshita M, Kuwabara Y, Marusawa H, Iwanaga Y, Hasegawa K, Yokode M, Kimura T, Kita T. MicroRNA-33 encoded by an intron of sterol regulatory element-binding protein 2 (Srebp2) regulates HDL in vivo. *Proc Natl Acad Sci USA*. 2010;107:17321–17326. doi: 10.1073/pnas.1008499107.
10. Ouimet M, Ediriweera HN, Gundra UM, et al. MicroRNA-33-dependent regulation of macrophage metabolism directs immune cell polarization in atherosclerosis. *J Clin Invest*. 2015;125:4334–4348. doi: 10.1172/JCI81676.
11. Rayner KJ, Esau CC, Hussain FN, et al. Inhibition of miR-33a/b in non-human primates raises plasma HDL and lowers VLDL triglycerides. *Nature*. 2011;478:404–407. doi: 10.1038/nature10486.
12. Raffort J, Lareyre F, Clement M, Mallat Z. Micro-RNAs in abdominal aortic aneurysms: insights from animal models and relevance to human disease. *Cardiovasc Res*. 2016;110:165–177. doi: 10.1093/cvr/cvw046.
13. Golledge J, van Bockxmeer F, Jamrozik K, McCann M, Norman PE. Association between serum lipoproteins and abdominal aortic aneurysm. *Am J Cardiol*. 2010;105:1480–1484. doi: 10.1016/j.amjcard.2009.12.076.
14. Mourmoura E, Vasilaki A, Giannoukas A, Michalodimitrakis E, Pavlidis P, Tsezou A. Evidence of deregulated cholesterol efflux in abdominal aortic aneurysm. *Acta Histochem*. 2016;118:97–108. doi: 10.1016/j.acthis.2015.11.012.
15. Zhao L, Jin H, Yang B, Zhang S, Han S, Yin F, Feng Y. Correlation between ABCA1 gene polymorphism and aopA-I and HDL-C in abdominal aortic aneurysm. *Med Sci Monit*. 2016;22:172–176. doi:10.12659/MSM.895298.
16. Wanhainen A, Mani K, Vorkapic E, De Basso R, Björck M, Länne T, Wågsäter D. Screening of circulating microRNA biomarkers for prevalence of abdominal aortic aneurysm and aneurysm growth. *Atherosclerosis*. 2017;256:82–88. doi: 10.1016/j.atherosclerosis.2016.11.007.
17. Daugherty A, Manning MW, Cassis LA. Angiotensin II promotes atherosclerotic lesions and aneurysms in apolipoprotein E-deficient mice. *J Clin Invest*. 2000;105:1605–1612. doi: 10.1172/JCI7818.
18. Manning MW, Cassi LA, Huang J, Szilvassy SJ, Daugherty A. Abdominal aortic aneurysms: fresh insights from a novel animal model of the disease. *Vasc Med*. 2002;7:45–54. doi: 10.1191/1358863x02vm413ra.
19. Daugherty A, Manning MW, Cassis LA. Antagonism of AT2 receptors augments angiotensin II-induced abdominal aortic aneurysms and atherosclerosis. *Br J Pharmacol*. 2001;134:865–870. doi: 10.1038/sj.bjp.0704331.
20. Cao RY, Amand T, Ford MD, Piomelli U, Funk CD. The murine angiotensin II-induced abdominal aortic aneurysm model: rupture risk and inflammatory progression patterns. *Front Pharmacol*. 2010;1:9. doi: 10.3389/fphar.2010.00009.
21. Longo GM, Xiong W, Greiner TC, Zhao Y, Fiotti N, Baxter BT. Matrix metalloproteinases 2 and 9 work in concert to produce aortic aneurysms. *J Clin Invest*. 2002;110:625–632. doi: 10.1172/JCI15334.
22. Wang Y, Krishna S, Golledge J. The calcium chloride-induced rodent model of abdominal aortic aneurysm. *Atherosclerosis*. 2013;226:29–39. doi: 10.1016/j.atherosclerosis.2012.09.010.
23. Sprague AH, Khalil RA. Inflammatory cytokines in vascular dysfunction and vascular disease. *Biochem Pharmacol*. 2009;78:539–552. doi: 10.1016/j.bcp.2009.04.029.
24. Yoshimura K, Aoki H, Ikeda Y, Fujii K, Akiyama N, Furutani A, Hoshii Y, Tanaka N, Ricci R, Ishihara T, Esato K, Hamano K, Matsuzaki M. Regression of abdominal aortic aneurysm by inhibition of c-Jun N-terminal kinase. *Nat Med*. 2005;11:1330–1338. doi: 10.1038/nm1335.
25. Yvan-Charvet L, Pagler TA, Seimon TA, Thorp E, Welch CL, Witztum JL, Tabas I, Tall AR. ABCA1 and ABCG1 protect against oxidative stress-induced macrophage apoptosis during efferocytosis. *Circ Res*. 2010;106:1861–1869. doi: 10.1161/CIRCRESAHA.110.217281.
26. Goebeler M, Kilian K, Gillitzer R, Kunz M, Yoshimura T, Bröcker EB, Rapp UR, Ludwig S. The MKK6/p38 stress kinase cascade is critical for tumor necrosis factor-alpha-induced expression of monocyte-chemoattractant protein-1 in endothelial cells. *Blood*. 1999;93:857–865.
27. Domoto K, Taniguchi T, Takaishi H, Takahashi T, Fujioka Y, Takahashi A, Ishikawa Y, Yokoyama M. Chylomicron remnants induce monocyte chemoattractant protein-1 expression via p38 MAPK activation in vascular smooth muscle cells. *Atherosclerosis*. 2003;171:193–200.
28. Barter PJ, Nicholls S, Rye KA, Anantharamaiah GM, Navab M, Fogelman AM. Antiinflammatory properties of HDL. *Circ Res*. 2004;95:764–772. doi: 10.1161/01.RES.0000146094.59640.13.
29. Ardans JA, Economou AP, Martinson JM Jr, Zhou M, Wahl LM. Oxidized low-density and high-density lipoproteins regulate the production of matrix metalloproteinase-1 and -9 by activated monocytes. *J Leukoc Biol*. 2002;71:1012–1018.
30. Tölle M, Pawlak A, Schuchardt M, Kawamura A, Tietge UJ, Lorkowski S, Keul P, Assmann G, Chun J, Levkau B, van der Giet M, Nofer JR. HDL-associated lysosphingolipids inhibit NAD(P)H oxidase-dependent monocyte chemoattractant protein-1 production. *Arterioscler Thromb Vasc Biol*. 2008;28:1542–1548. doi: 10.1161/ATVBAHA.107.161042.
31. Aiello RJ, Brees D, Bourassa PA, Royer L, Lindsey S, Coskran T, Haghpassand M, Francone OL. Increased atherosclerosis in hyperlipidemic mice with inactivation of ABCA1 in macrophages. *Arterioscler Thromb Vasc Biol*. 2002;22:630–637.
32. Tang C, Liu Y, Kessler PS, Vaughan AM, Oram JF. The macrophage cholesterol exporter ABCA1 functions as an anti-inflammatory receptor. *J Biol Chem*. 2009;284:32336–32343. doi: 10.1074/jbc.M109.047472.
33. Steinmetz EF, Buckley C, Shames ML, Ennis TL, Vanvickle-Chavez SJ, Mao D, Goeddel LA, Hawkins CJ, Thompson RW. Treatment with simvastatin suppresses the development of experimental abdominal aortic aneurysms in normal and hypercholesterolemic mice. *Ann Surg*. 2005;241:92–101.
34. Shiraya S, Miyake T, Aoki M, Yoshikazu F, Ohgi S, Nishimura M, Ogihara T, Morishita R. Inhibition of development of experimental aortic abdominal aneurysm in rat model by atorvastatin through inhibition of macrophage migration. *Atherosclerosis*. 2009;202:34–40. doi: 10.1016/j.atherosclerosis.2008.03.020.
35. Obad S, dos Santos CO, Petri A, Heidenblad M, Broom O, Ruse C, Fu C, Lindow M, Stenvang J, Straarup EM, Hansen HF, Koch T, Pappin D, Hannon GJ, Kauppinen S. Silencing of microRNA families by seed-targeting tiny LNAs. *Nat Genet*. 2011;43:371–378. doi: 10.1038/ng.786.
36. van Rooij E, Kauppinen S. Development of microRNA therapeutics is coming of age. *EMBO Mol Med*. 2014;6:851–864. doi: 10.15252/emmm.201100899.
37. Niesor EJ, Schwartz GG, Perez A, Stauffer A, Durrwell A, Bucklar-Suchankova G, Benghozi R, Abt M, Kallend D. Statin-induced decrease in ATP-binding cassette transporter A1 expression via microRNA33 induction may counteract cholesterol efflux to high-density lipoprotein. *Cardiovasc Drugs Ther*. 2015;29:7–14. doi:10.1007/s10557-015-6570-0.

Highlights

- Abdominal aortic aneurysm (AAA) is increasingly prevalent, and its growth results in fatal rupture. Although asymptomatic diagnosis by penetrating computed tomography scans is becoming more common, drugs to prevent AAA growth are thus far unavailable.
- miR (microRNA)-33a-5p expression in central zone of human AAA was higher than marginal zone. MiR deletion ameliorated AAA formation both in calcium chloride– and angiotensin II–induced AAA models in mice. Death from AAA rupture was also reduced.
- The mechanisms identified include attenuated c-Jun N-terminal kinase activation in miR-33$^{-/-}$ macrophages, p38 mitogen-activated protein kinase activation in miR-33$^{-/-}$ vascular smooth muscle cells, and augmented anti-inflammatory effect of high-density lipoprotein from miR-33$^{-/-}$ mice, resulting in reduced matrix metalloproteinase 9, monocyte chemotactic protein-1 expression in macrophages and vascular smooth muscle cells.
- Our findings indicate that inhibition of miR-33 may be a novel strategy for the treatment of AAA.

Arteriosclerosis, Thrombosis, and Vascular Biology

Journal of the American Heart Association

Genetic Ablation of MicroRNA-33 Attenuates Inflammation and Abdominal Aortic Aneurysm Formation via Several Anti-Inflammatory Pathways

Tetsushi Nakao, Takahiro Horie, Osamu Baba, Masataka Nishiga, Tomohiro Nishino, Masayasu Izuhara, Yasuhide Kuwabara, Hitoo Nishi, Shunsuke Usami, Fumiko Nakazeki, Yuya Ide, Satoshi Koyama, Masahiro Kimura, Naoya Sowa, Satoko Ohno, Hiroki Aoki, Koji Hasegawa, Kazuhisa Sakamoto, Kenji Minatoya, Takeshi Kimura and Koh Ono

Arterioscler Thromb Vasc Biol. 2017;37:2161-2170; originally published online September 7, 2017;
doi: 10.1161/ATVBAHA.117.309768
Arteriosclerosis, Thrombosis, and Vascular Biology is published by the American Heart Association, 7272 Greenville Avenue, Dallas, TX 75231

Print ISSN: 1079-5642. Online ISSN: 1524-4636

SUPPLEMENTAL MATERIAL

Genetic Ablation of MicroRNA-33 Attenuates Inflammation and Abdominal Aortic Aneurysm Formation via Several Anti-inflammatory Pathways

Tetsushi Nakao, MD[1]; Takahiro Horie, MD, PhD[1]; Osamu Baba, MD, PhD[1]; Masataka Nishiga, MD[1]; Tomohiro Nishino, MD, PhD[1]; Masayasu Izuhara, MD[1]; Yasuhide Kuwabara, MD, PhD[1], Hitoo Nishi, MD, PhD[1]; Shunsuke Usami, MD, PhD[1]; Fumiko Nakazeki, MD[1]; Yuya Ide, MD[1]; Satoshi Koyama, MD[1]; Masahiro Kimura, MD[1]; Naoya Sowa[1]; Satoko Ohno, MD, PhD[2]; Hiroki Aoki, MD, PhD[2]; Koji Hasegawa, MD, PhD[3]; Takeshi Kimura, MD, PhD[1]; Koh Ono, MD, PhD[1]

Supplemental Table

Supplemental Table 1. Primer sequences for quantitative real-time PCR

Species	Gene	Forward primer	Reverse primer
Human	*MMP9*	TTGACAGCGACAAGAAGTGG	GCCATTCACGTCGTCCTTAT
	GAPDH	AAATTCCATGGCACCGTCAA	AGGGATCTCGCTCCTGGAA
Mouse	*Il-1β*	TCAGGCAGGCAGTATCACTCA	GGAAGGTCCACGGGAAAGAC
	Il-10	AAATAAGAGCAAGGCAGTGGAG	TCATTCATGGCCTTGTAGACAC
	Mmp2	ATCTTTGCAGGAGACAATGGCTG	TTCAGGTAATAAGCACCCTTGAA
	Mmp9	TCACACGACATCTTCCAGTACC	CACCTCATTTTGGAAACTCACA
	Jnk1	GCTGTGTGGAATCAAGCACC	AGCGAGTCACCACATAAGGC
	MCP-1 (*Ccl2*)	CTGGATCGGAACCAAATGAG	TGAGGTGGTTGTGGAAAAGG
	Tnfa	CCAGACCCTCACACTCAGATC	CACTTGGTGGTTTGCTACGAC
	Arg1	AACTCTTGGGAAGACAGCAGAG	GTAGTCAGTCCCTGGCTTATGG
	Fizz	AGGATGCCAACTTTGAATAGGA	AGTTAGCTGGATTGGCAAGAAG
	Gapdh	TTGCCATCAACGACCCCTTC	TTGTCATGGATGACCTTGGC
Rat	MCP-1 (*Ccl2*)	AGGTGTCCCAAAGAAGCTGT	GGTGCTGAAGTCCTTAGGGT
	Gapdh	TTGCCATCAACGACCCCTTC	TTGTCATGGATGACCTTGGC

Supplemental Figures and Legends

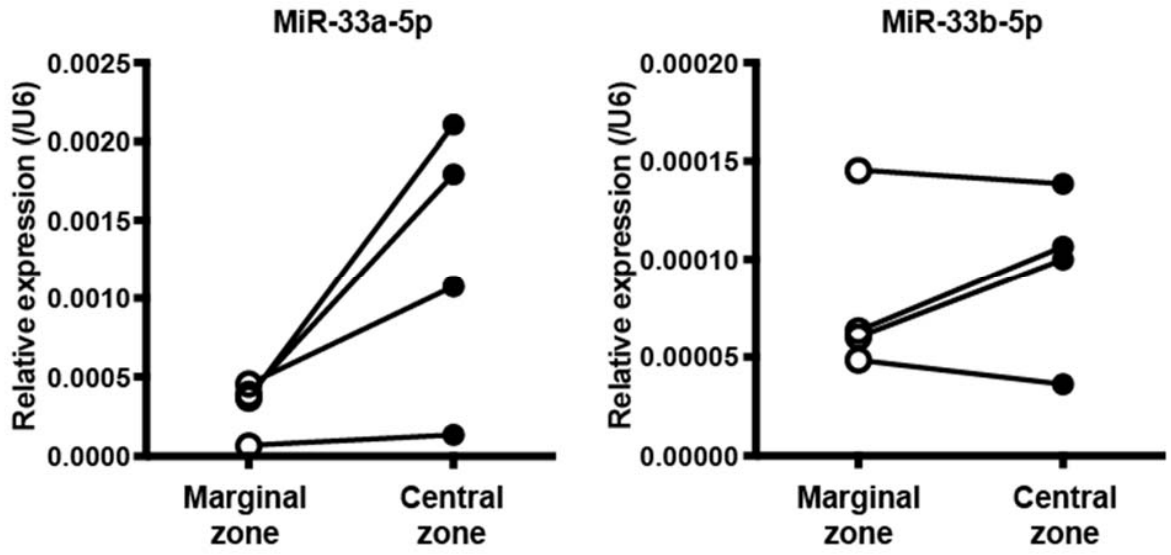

Supplemental Figure I. Human abdominal aortic aneurysm samples obtained during the artificial graft replacement procedures were analyzed by quantitative real-time PCR and central zone and marginal zone were compared in each sample. MiR-33 indicates microRNA-33.

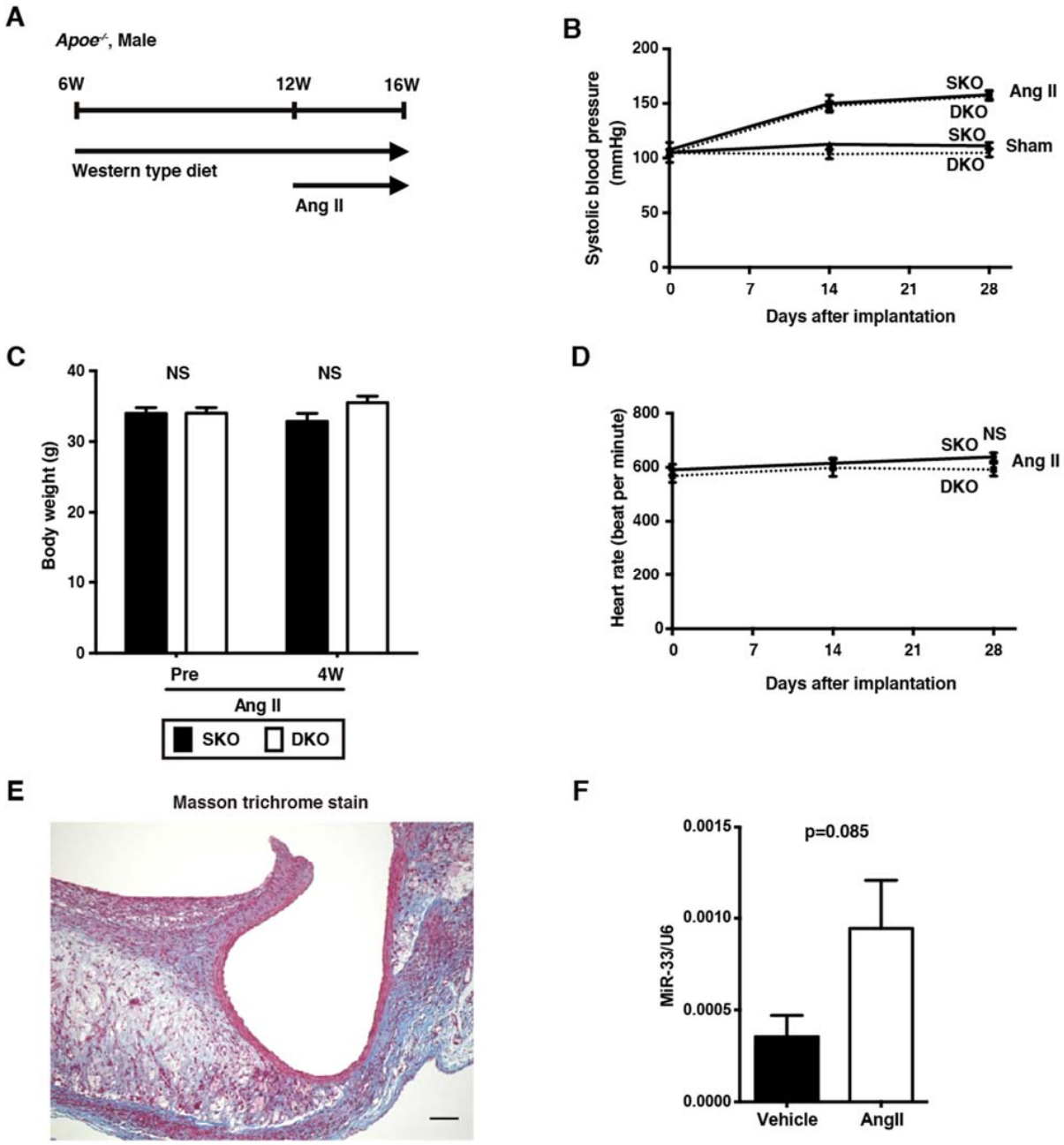

Supplemental Figure II. A, Scheme of Angiotensin (Ang)II-induced abdominal aortic aneurysm (AAA) experiments. *Apoe*$^{-/-}$ background mice were fed a Western-Type Diet from 6 weeks old. At 12 weeks old, subcutaneous continuous infusion of 1 μg/kg/min AngII was performed for 4 weeks. Mice were perfused by saline and 4% paraformaldehyde and dissected aortas were analyzed. **B.** Systolic blood pressure of microRNA (miR)-33$^{+/+}$*Apoe*$^{-/-}$ (single knockout [SKO]) and miR-33$^{-/-}$*Apoe*$^{-/-}$ (double knockout [DKO]) mice pre and post AngII treatment. There was no significant difference between groups assessed by two-way analysis of variance (ANOVA) with Tukey's multiple comparison test, n=8–10 mice/group. **C,** Body weight of SKO and DKO mice pre and post AngII treatment. There is no significant differences between groups assessed by two-way ANOVA with Tukey's multiple comparison test. N=13–15 for the pre group, and n=9 each for the post group because some mice died of aortic rupture. **D,** Heart rate of SKO and DKO mice pre and post AngII treatment. There is no significant difference between groups assessed by two-way ANOVA with Tukey's multiple comparison test, n=8–10 mice/group. **E,** MiR-33 expression in AngII treated and vehicle (saline)-treated mice at suprarenal abdominal aortic lesion. Student's t-test, n=4. **F,** High

magnification (×100) of Masson trichrome of SKO in Figure 1C indicating dissected media and pseudolumen. The black bar indicates 100 μm. All data represent means ± standard error of mean.

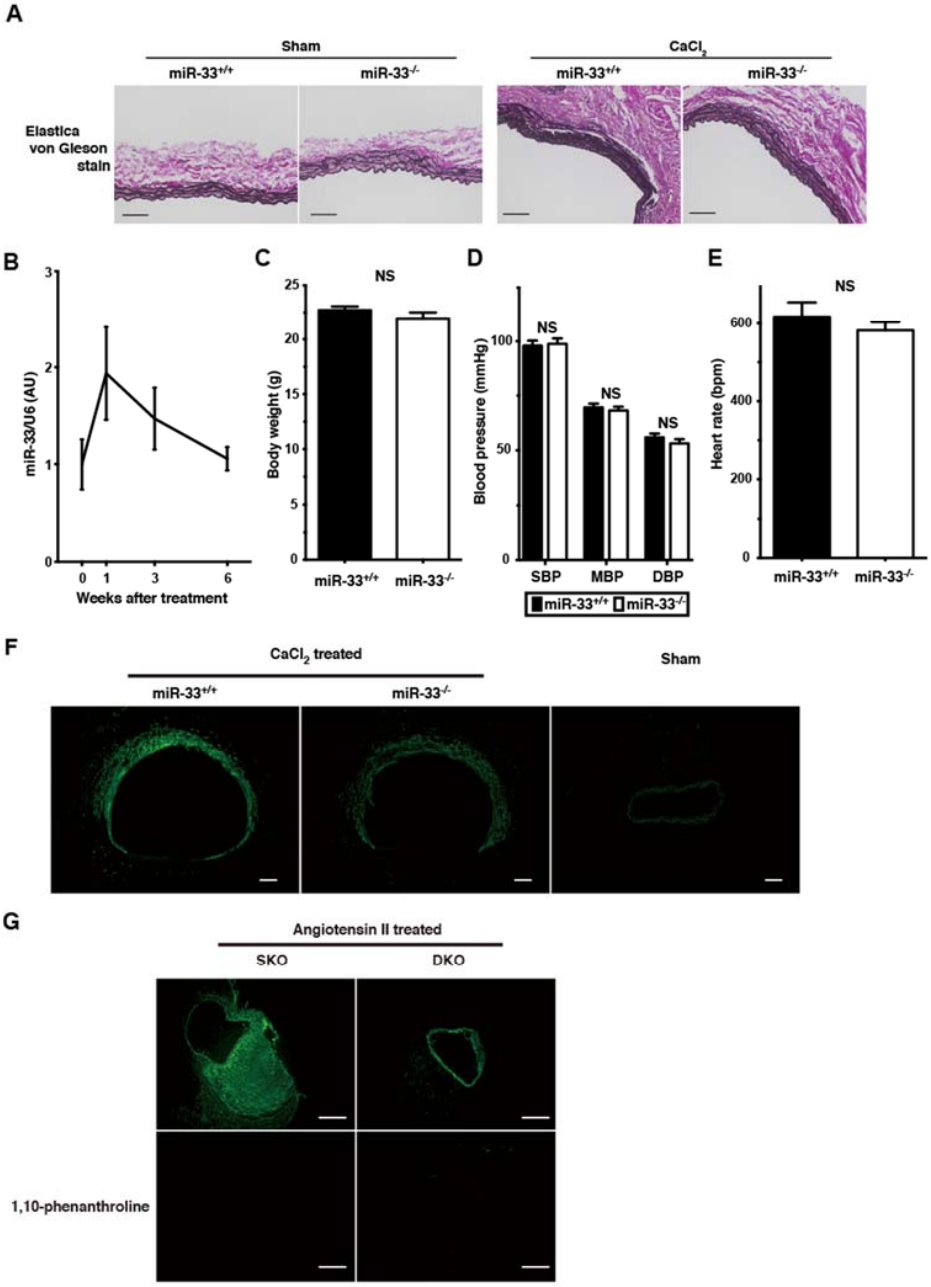

Supplemental Figure III. A, Representative images of Elastica van Gieson (EVG) stained aortic sections from sham and calcium chloride ($CaCl_2$)-treated microRNA (miR)-33$^{+/+}$ and miR-33$^{-/-}$ mice. Black bars are scale bars of 100 μm. **B,** MiR-33 is upregulated after abdominal aortic aneurysm (AAA) induction by periaortic $CaCl_2$ application. MiR-33 expression in the AAA wall after 1, 3, and 6 weeks after $CaCl_2$ application assessed by quantitative real-time PCR using TaqMan Probes. **C~E,** No significant difference between miR-33$^{+/+}$ and miR-33$^{-/-}$ mice in baseline data of $CaCl_2$-induced AAA model. Body weight (**C**, assessed by Student's t-test), blood pressure (**D**, assessed by two-way analysis of variance with Tukey's multiple comparison test) and heart rate (**E**, assessed by Student's t-test) 6 weeks after $CaCl_2$ application. n=10. **F,** Representative in situ zymography of $CaCl_2$ induced AAA in miR-33$^{+/+}$ and miR-33$^{-/-}$ mice (×100). Sham operated aorta of a wild-type mice was used as negative control. The white bars represent scale bar of 500 μm. All data represent means ± standard error of mean. **G.** Representative in situ zymography of Angiotensin II-induced AAA in single knockout (SKO) and double knockout (DKO) mice (×40). 1,10-phenanthroline was used as a negative control. The white bars indicate 500 μm. AU, indicates

arbitrary unit; DBP, diastolic blood pressure; MBP, mean blood pressure; NS, not significant; SBP, systolic blood pressure.

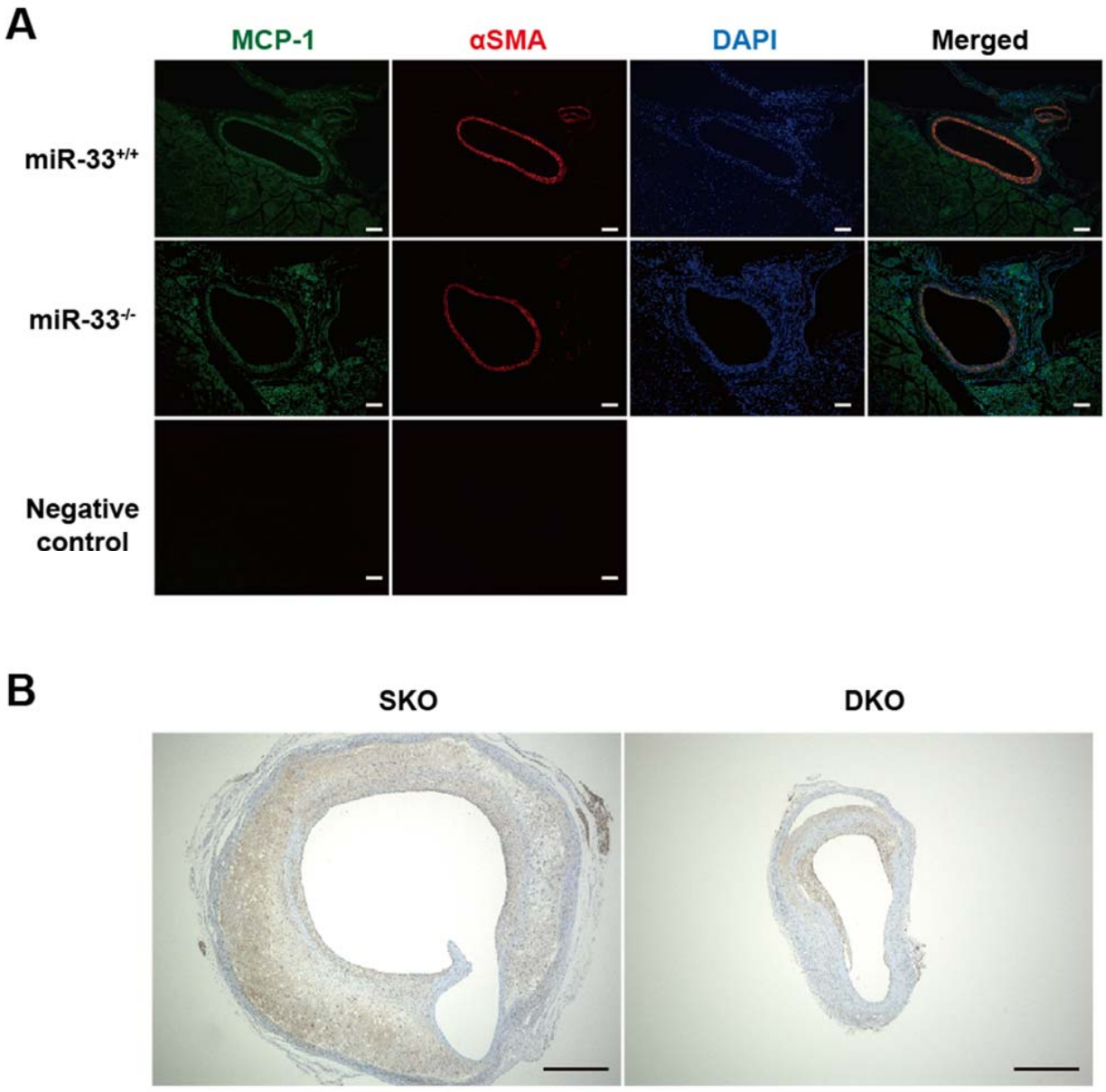

Supplemental Figure IV. A. MCP-1 and alpha smooth muscle actin (αSMA) were assessed by immunohistochemistry in micro-RNA (miR)-33$^{+/+}$ and miR-33$^{-/-}$ aortas (×100). The white bars indicate 100 μm. **B.** Immunohistochemistry of Monocyte chemotactic protein-1 (MCP-1) in Angiotensin II-induced abdominal aortic aneurysm (×40). Scale bars indicate 500 μm. DAPI indicates 4',6-diamidino-2-phenylindole; DKO, double knockout; SKO, single knockout.

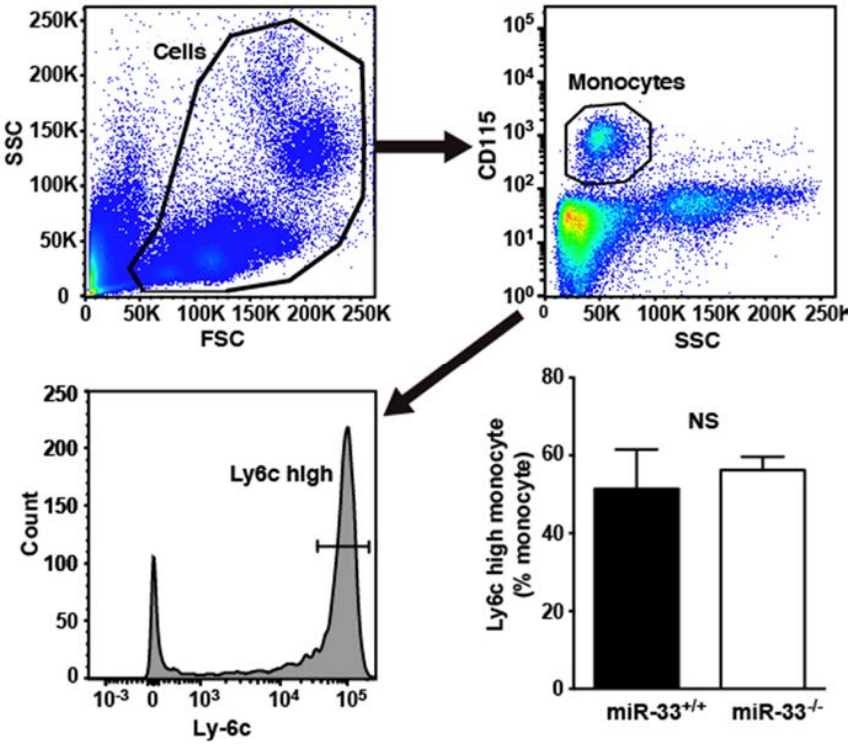

Supplemental Figure V. Peripheral blood of calcium chloride ($CaCl_2$)-treated microRNA (miR)-33$^{-/-}$ mice revealed no significant difference in the numbers of Ly-6c^{high} monocytes. Peripheral blood obtained from miR-33$^{+/+}$ and miR-33$^{-/-}$ mice 7 days after $CaCl_2$ application were analyzed by flow cytometry. CD115^{+}, SSC^{low} cells were defined as monocytes (upper right panel). The percentage of Ly-6c^{high} monocytes (lower left panel) per total number of monocytes was not significantly different between groups (lower right panel), assessed by Student's t-test, n=9–11. All data represent means ± standard error of mean.

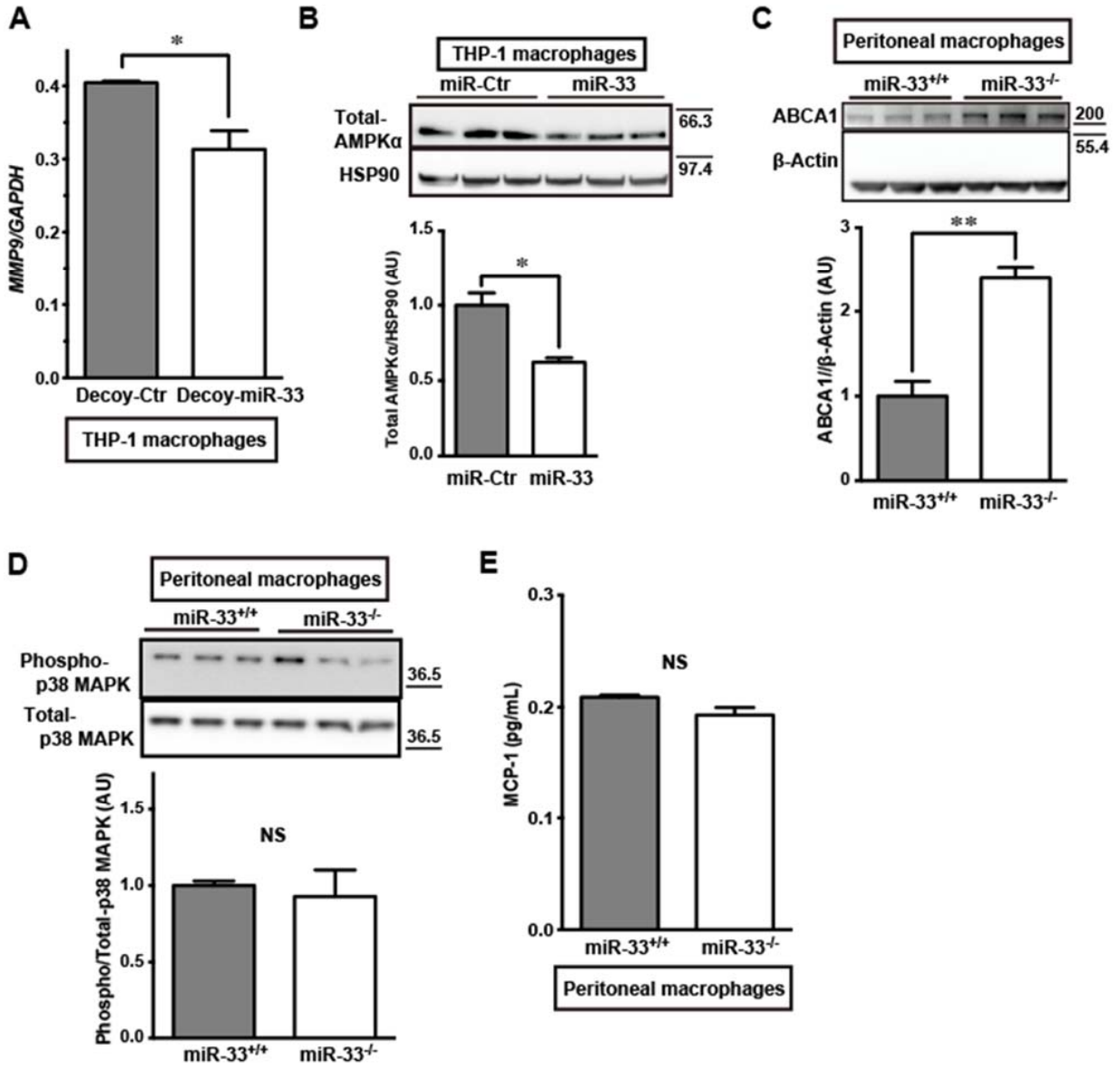

Supplemental Figure VI. A, Knockdown of microRNA (miR)-33 in THP-1 macrophages reduced matrix metalloproteinase (MMP) 9 mRNA expression. Student's t-test, n=3. **B,** Overexpression of miR-33 in THP-1 macrophages reduced AMP-activated protein kinase α1 (AMPKα) expression. Student's t-test, n=3. **C,** ATP binding cassette transporter A1 (ABCA1) expression in miR-33$^{-/-}$ peritoneal macrophages were elevated than miR-33$^{+/+}$ peritoneal macrophages. Student's t-test, n=3. **D.** P38 mitogen-activated protein kinase (MAPK) activity was not different between miR-33$^{+/+}$ and miR-33$^{-/-}$ peritoneal macrophages, assessed by Student's t-test, n=6. **E,** Monocyte chemotactic protein 1 (MCP-1) expression in peritoneal macrophages was not different between miR-33$^{+/+}$ and miR-33$^{-/-}$. n=3. All data represent means ± standard error of mean. All data were assessed by Student's t-test, *; P<0.05, **; P<0.01. AU indicates arbitrary unit; HSP90, heat shock protein 90; NS, not significant.

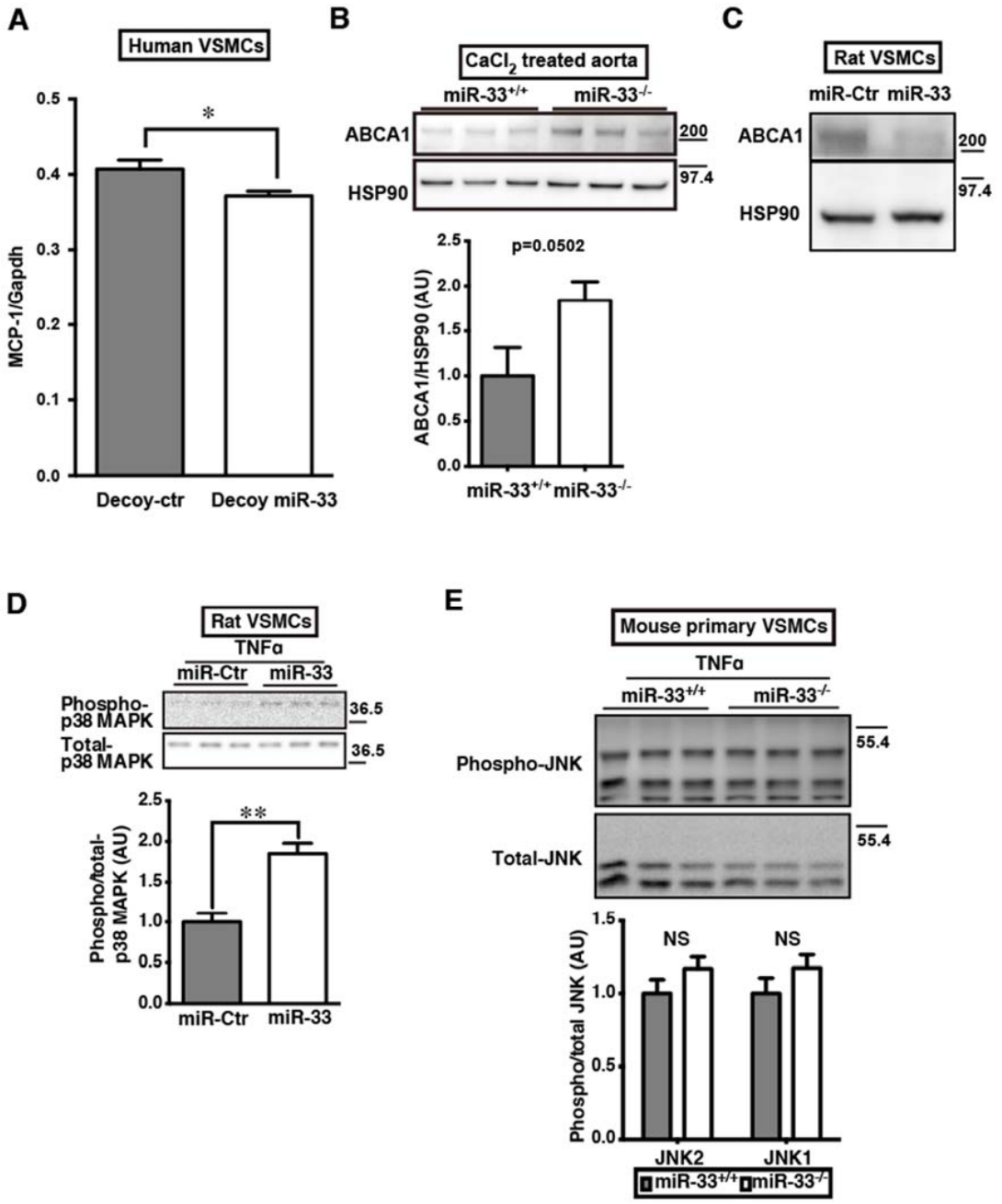

Supplemental Figure VII. A, Human vascular smooth muscle cells (VSMCs) were transfected with decoy-miR-33 or its control, and assessed by quantitative real-time PCR (qRT-PCR) analyses. **B,** Calcium chloride ($CaCl_2$)-induced abdominal aortic aneurysm (AAA) in microRNA (miR)-$33^{+/+}$ and miR-$33^{-/-}$ mice were assessed by western blotting. P values were assessed by Student's t-test, n=6. **C,** Rat VSMCs were transfected by miR-33 or control and assessed by western blotting. **D,** MiR-33 over expression activates p38 mitogen-activated protein kinase (MAPK) in rat VSMCs. MiR-33 and control miR were over expressed in rat VSMCs using lentiviral infection and assessed by qRT-PCR. ** denotes P<0.01 assessed by Student's t-test, n=3. This is a representative of three biological replicates. **E,** Western blotting analysis of c-Jun N-terminal kinase (JNK) in mouse VSMCs stimulated by 25 ng/mL tissue necrosis factor (TNF) α for 15 min. Data were assessed by two-way analysis of variance (ANOVA) with Tukey's multiple comparison test, n=3. All data represent means ± standard error of mean. ABCA1 indicates ATP-binding cassette transporter A1; AU, arbitrary unit; MCP-1, monocyte chemotactic protein-1; HSP90, heat shock protein 90.

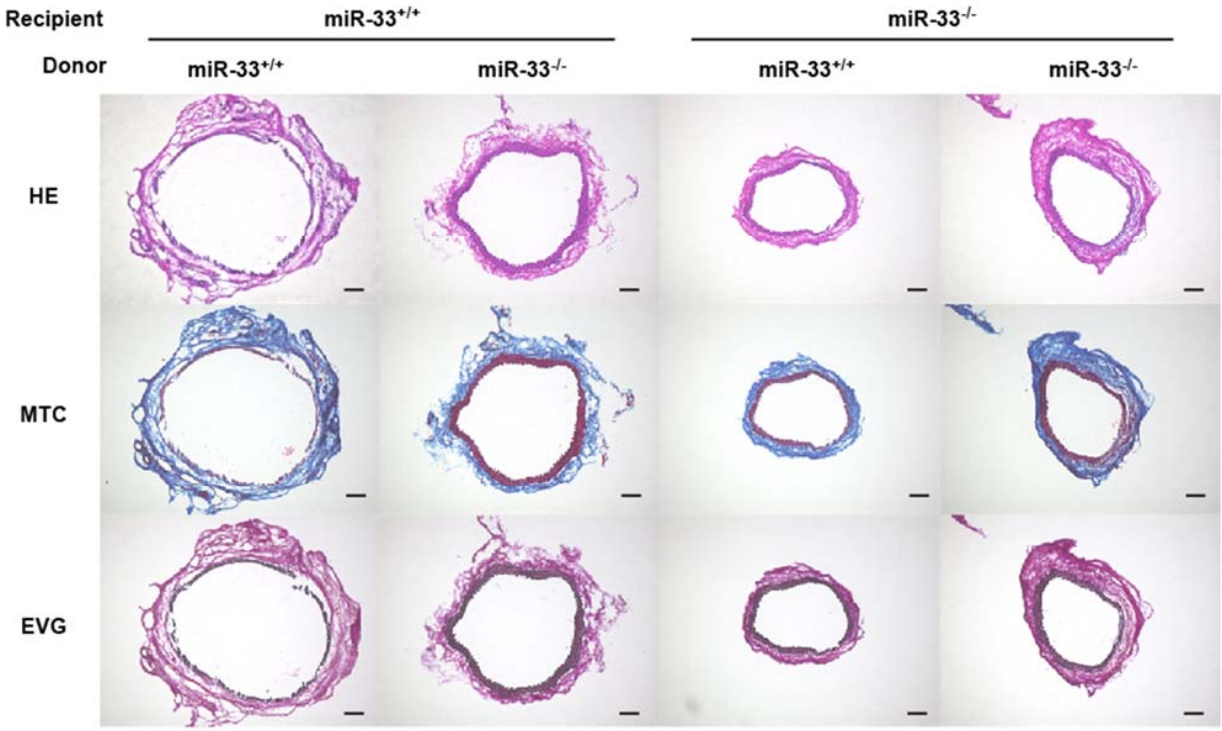

Supplemental Figure VIII. Histochemical analysis of calcium chloride-induced abdominal aortic aneurysm in bone marrow transplantation experiments (×40). The black bars indicate scale bars of 500 μm. EVG indicates Elastica van Gieson staining; HE, hematoxylin-eosin; miR-33, microRNA-33; MTC, Masson trichrome.

SUPPLEMENTAL MATERIAL

Genetic Ablation of MicroRNA-33 Attenuates Inflammation and Abdominal Aortic Aneurysm Formation via Several Anti-Inflammatory Pathways

Tetsushi Nakao, MD[1]; Takahiro Horie, MD, PhD[1]; Osamu Baba, MD, PhD[1]; Masataka Nishiga, MD[1]; Tomohiro Nishino, MD, PhD[1]; Masayasu Izuhara, MD[1]; Yasuhide Kuwabara, MD, PhD[1], Hitoo Nishi, MD, PhD[1]; Shunsuke Usami, MD, PhD[1]; Fumiko Nakazeki, MD[1]; Yuya Ide, MD[1]; Satoshi Koyama, MD[1]; Masahiro Kimura, MD[1]; Naoya Sowa[1]; Satoko Ohno, MD, PhD[2]; Hiroki Aoki, MD, PhD[2]; Koji Hasegawa, MD, PhD[3]; Kazuhisa Sakamoto, MD[4]; Kenji Minatoya, MD, PhD[4]; Takeshi Kimura, MD, PhD[1]; Koh Ono, MD, PhD[1]

Detailed Materials and Methods

Humna samples of abdominal aortic aneurysms (AAA)

Human AAA samples were collected during the artificial blood vessel replacement surgery, when written permission from patients could have been obtained before the procedures. Tissues were soaked in RNA later (Invitrogen) at 4 °C overnight, then stored at -80°C. Tripure Reagent (Roche) and polytron homogenizer (Microtec) were used to extract RNA. All procedures conformed to the tenets of the Declaration of Helsinki. This study was approved by Institutional Review Board/Ethics Committee of the Kyoto University Graduate School of Medicine (No. G473)

Animals

MiR-33$^{-/-}$ and miR-33$^{-/-}$ apolipoprotein E *(Apoe)*$^{-/-}$ (double-knockout; DKO) mice were generated as described previously.[1,2] MiR-33$^{+/+}$ or miR-33$^{+/+}$*Apoe*$^{-/-}$ (single-knockout; SKO) littermates were used as controls. Every strain used was C57BL/6 background.

For angiotensin II (AngII)–induced abdominal aortic aneurysm (AAA), we modified a previously reported protocol.[3] *Apoe*$^{-/-}$ background mice (SKO and DKO) were fed a Western-type diet containing 0.15% cholesterol and 20% fat (Oriental Yeast) from 6 weeks of age, and AngII (1 μg/min/kg) was infused continuously using subcutaneously implanted osmotic pumps (Mini-Osmotic Pump Model 2004, Alzet) for 4 weeks from 12 to 16 weeks of age.

For the calcium chloride ($CaCl_2$)-induced AAA model, periaortic application of $CaCl_2$ was performed as previously described.[4] Briefly, mice were anesthetized (intraperitoneal injection of pentobarbital 80 mg per kg body weight at a concentration of 6.5 mg/mL) and underwent laparotomy at age 7–8 weeks. The abdominal aorta between the renal arteries and bifurcation of the iliac arteries was isolated from the surrounding retroperitoneal structures. Then, 0.5 mol/L of $CaCl_2$ was applied to the external surface of the aorta. Saline was substituted for $CaCl_2$ in sham control mice. After 20 minutes, the aorta was rinsed with saline and the incision was closed. AAA diameter was assessed 6 weeks after the procedure. For surgical procedures, mice were anesthetized by intraperitoneal injection of pentobarbital 80 mg per kg body weight at a concentration of 6.5 mg/mL.

Mice were sacrificed by intraperitoneal injection of a sufficient amount of pentobarbital, and perfused with phosphate-buffered saline (PBS) and subsequently with 4% paraformaldehyde at physiological pressure. Abdominal aortas were excised using microscissors. To determine the external diameter, we photographed the specimen in PBS to avoid collapse of the vasculature, and the specimens were then used in histological analyses. Aneurysm severity in the AngII model was assessed

using the scoring system described by Daugherty *et al* (2001): type 0, no aneurysm (the suprarenal region of the aorta was not obviously different from that in naïve *Apoe*$^{-/-}$ mice without AngII treatment); type I, dilated lumen with no thrombus; type II, remodeled tissue often containing thrombus; type III, a pronounced bulbous form of type II containing thrombus; and type IV, multiple aneurysms containing thrombi.[5]

Blood pressure and heart rate were measured using a noninvasive tail cuff system (BP-98A, Softron).

All mice were maintained in specific-pathogen-free laboratories at Kyoto University Graduate School of Medicine. This investigation was performed with the approval of the Kyoto University Ethics Review Board.

Bone Marrow Transplantation

BM transplantation was conducted as described previously.[6,7] Male mice with genotypes of miR-33$^{+/+}$ and miR-33$^{-/-}$ (8–9 weeks old) were used as BM donors. BM recipients were female miR-33$^{+/+}$ mice and miR-33$^{-/-}$ mice (8 weeks old). BM donors were euthanized by cervical dislocation, and BM cells were collected by flushing femurs and tibias with PBS supplemented with 2% fetal bovine serum (FBS). The suspension was passed through 40-μm nylon mesh. Red blood cells were lysed using ACK lysing buffer (Lonza). BM cells were then washed twice with PBS supplemented with 2% FBS. Recipients were irradiated with two doses of 6 Gy within an interval of 3 hours (cesium 137; Gammacell 40 Exactor) and injected intravenously with 2×10^6 BM cells 6 hours after irradiation. Six weeks after bone marrow transplantation, AAA was induced by $CaCl_2$ application as mentioned above. AAA diameter and serum HDL-C were assessed 6 weeks after the operation.

Cell Culture and Reagents

Peritoneal macrophages were obtained from the peritoneal cavity of mice 4 days after intraperitoneal injection of 3 mL of 3% thioglycollate. The cells obtained were washed, spun at 1,000 rpm for 5 minutes, and plated at a density of 1.0×10^6 cells/mL in RPMI1640 medium (Nacalai Tesque) containing 10% FBS. Recombinant tumor necrosis factor α (TNFα; 25 ng/mL; R&D) with or without SP600125 (100 μmol/L; Sigma) was used to stimulate macrophages.

THP-1 cells were purchased from the American Type Cell Collection. THP-1 macrophages were transfected by lentivirus and transformed into macrophages by incubation for 3 days with 100nM PMA (Nacalai Tesque)

Mouse aortic VSMCs were obtained from the thoracic aortas of 8- to 12-week-old miR-33$^{+/+}$ or miR-33$^{-/-}$ mice. Adventitia and endothelium were removed after digestion of the aortic segments with collagenase type II (175 units/mL; Worthington). The media were further digested with a mixture containing collagenase type II (175 units/mL) and elastase (0.5 mg/mL; Sigma), which yielded 100,000 cells per aorta. Cells were grown on gelatin-coated dishes in Dulbecco's modified Eagle's medium containing 10% FBS, 100 units/mL penicillin, and 100 μg/mL streptomycin, and incubated at 37°C with 5% CO_2 / 95% air. All the following experiments involving mouse aortic VSMCs were performed using cells with a passage number of 5. SB203580 (p38 MAPK inhibitor) was purchased from Sigma and used at a concentration of 20 μmol/L for incubation with VSMCs.

Primary human aortic VSMCs were purchased from Kurabo and cultured in medium provided by the manufacturer. VSMCs were seeded on 6 well plate at the concentration of $2.5x10^5$ per well, and transfected by lentivirus on the next day.

For HDL-C experiments, human HDL-C (BT-914) was obtained from ThermoFisher Scientific Chemicals. Serum HDL-C fragments were isolated using a

polyethylene glycol (PEG) method, as described previously.[1] Serum collected from miR-33$^{+/+}$ and miR-33$^{-/-}$ mice using blood separator tubes (Bloodsepar, IBL) was treated with a 40% volume of PEG for 20 min at room temperature, and centrifuged at 10,000g for 30 min at 4°C, and then the supernatant was collected as the HDL-C fragment (PEG-HDL). Peritoneal macrophages and primary VSMCs were incubated with or without PEG-HDL or human HDL-C for 4.5 hours, and peritoneal macrophages were subsequently stimulated with TNFα (25 ng/mL) for 3 hours.

For LNA transfection into peritoneal macrophages, Lipofectamine 2000 (Invitrogen) was used according to the manufacturer's instruction. LNA of mouse siAMPKα1 (s98536) and its control (4390843) was purchased from Applied Biosystems. LNA for siABCA1 were designed by siDirect (http://sidirect2.rnai.jp/) and purchased from Genedesign.

Lentivirus Production and DNA Transduction

We produced lentiviral stocks in 293T cells as described previously.[8] Cells were used for analyses 3 days after transduction. Expression vectors for the negative control (miR-control) and miRs were generated using a BLOCK-iT PolIImiR RNAi Expression Vector Kit in accordance with the manufacturer's protocol (Invitrogen). The miR-control vector contained the same hairpin structure as that in a regular pre-miR; this sequence is predicted not to target any known vertebrate gene (pcDNA6.2-GW/EmGFP-miR-neg control plasmid). To create an anti-miR-33 (decoy) vector, the luciferase 3′ untranslated region was modified to include six tandem sequences complementary to miR-33, separated by a single nucleotide spacer. The sequences of all constructs were analyzed using an ABI 3100 genetic analyzer. All of these constructs were correctly inserted into a pLenti6/V5-D-TOPO vector (Invitrogen) driven by a cytomegalovirus promoter to stably express genes in THP-1 cells and VSMCs.

Protein Extraction and Western Blotting

Mice were perfused with cold PBS at physiological pressure, and aortic specimens were dissected using microscissors. After being washed in cold PBS, they were homogenized in RIPA buffer (Nacalai Tesque). We determined protein concentrations in the samples using a BCA protein assay kit (Pierce).

For *in vitro* experiments, cultured cells were homogenized in lysis buffer consisting of 100 mmol/L Tris-HCl, 75 mmol/L NaCl, and 1% Triton X-100 at pH 7.4 (Nacalai Tesque). The buffer was supplemented with Complete Mini protease inhibitor (Roche), 0.5 mmol/L NaF, and 10 μmol/L $NaVO_4$ just prior to use. The protein concentration was determined by the Bradford method using Protein Assay Dye Reagent Concentrate (Bio-Rad, #500-0006).

Western blotting was performed using standard procedures as described previously.[1] A total of 1–10 μg of protein was fractionated using NuPAGE 4–12% Bis-Tris gels (Invitrogen) and transferred to a nitrocellulose transfer membrane (Whatman). The membrane was blocked using PBS containing 5% nonfat milk for 30 minutes and incubated with primary antibody of 1:1,000 overnight at 4°C. Anti-phospho-SAPK/JNK (#9251), anti-SAPK/JNK (#9252), anti-phospho-p38 MAPK (#9211s), and anti-p38 MAPK (#9212) antibodies were purchased from Cell Signaling. Anti-β-actin antibodies were from Sigma (A5441). After a washing step in PBS-0.05% Tween 20 (0.05% T-PBS), the membrane was incubated with a secondary antibody (anti-rabbit or anti-mouse IgG HRP-linked, 1:2,000) for 30 minutes at room temperature. The membrane was then washed in 0.05% T-PBS and detected by Immobilon Western HRP Substrate

(Millipore) using an ImageQuant LAS 4000 mini bimolecular imager (GE Healthcare Bio-Sciences AB). Obtained images were analyzed using ImageJ 1.46r (Wayne Rasband, National Institutes of Health).

Gelatin Zymography

Gelatin zymography was conducted as reported previously.[9] Conditioned media concentrated using a centrifugal filter device (Amicon Ultra NMWL 10K, Milipore) at 14,000 g for 10 minutes or extracted protein was treated with sample buffer (#LC2676, Invitrogen), and separated by electrophoresis with 10% gelatin containing Zymogram Gel (#EC61752BOX, Invitrogen) in Tris-Glycine SDS running buffer (#LC2675, Invitrogen). The gels were washed several times by distilled water, and incubated in renaturing buffer (#LC2670, Invitrogen,) for 30 minutes at room temperature with gentle agitation. Then, the gels were incubated at 37°C in developing buffer (#LC2670, Invitrogen) for 24 hours. After incubation, the gels were stained by Coomassie G-250 (SimplyBlue SafeStain; #LC6060, Invitrogen,), and analyzed using a LAS-3000 image analyzer (GE Healthcare Bio-Sciences AB). In situ zymography were conducted according to the previous report. [10-12] Breifly, unfixed cryostat sections (10μm thick) were incubated with 10 μg/ml DQ-gelatin (D12054, Molecular Probes) for 3 hours at 37℃. Fluorescence was detected with BZ-9000 (Keyence). 1,10-phenanthroline was used as an inhibitor of MMPs for negative control.

Monocyte Chemotactic Protein -1 Enzyme-Linked Immunosorbent Assay

Concentrations of monocyte chemotactic protein (MCP)-1 in the AAA wall and conditioned media were determined using an enzyme-linked immunosorbent assay (ELISA) kit (R&D Systems) in accordance with the manufacturer's instructions. Proteins in the AAA wall were collected as described above, and 20 μL was used for MCP-1 ELISA and standardized by protein amount. Serum-free conditioned media of peritoneal macrophages and VSMCs grown in 6-well plates for 3 days was collected and used for MCP-1 ELISA and standardized by the protein amount collected from the cells.

RNA Extraction and Quantitative Real-Time PCR

Total RNA was isolated and purified using TRI reagent (T9424, Sigma Aldrich) in accordance with the manufacturer's instructions. Then cDNA was synthesized from 1 μg of total RNA using a Verso cDNA Synthesis Kit (#AB-1453/B, Thermo Scientific) in accordance with the manufacturer's instructions. For quantitative real-time PCR (qRT-PCR), specific genes were amplified using 40 cycles with SYBR Green PCR Master Mix (Toyobo). Expression was normalized to the housekeeping gene *Gapdh*. Gene-specific primers are summarized in Supplemental Table 1.

MiR-33 and *U6* snRNA was measured in accordance with the TaqMan MicroRNA Assay (Applied Biosystems) protocol, and the products were analyzed using a thermal cycler (Prism7900HT sequence detection system, ABI). Samples were normalized by *U6* snRNA expression.

Flow Cytometry

Peripheral blood was collected from the orbital sinuses using heparin-coated capillary tubes. Total leukocytes were quantified from whole blood using a hematology cell counter (Celltac α MEK-6358, Nihon Kohden). Erythrocytes were lysed using a commercial RBC lysis solution (PharmLyse, BD Biosciences). Monocytes were identified by staining with an anti-CD115-antibody conjugated with Alexa Fluor 488 (clone AFS98, eBioscience), and monocyte subsets were identified by staining with an

anti-Ly-6c antibody conjugated with allophycocyanin (APC) (clone HK1.4, eBioscience). Data were acquired using a BD FACS Aria Flow Cytometer and analyzed with BD FACS Diva software (BD Biosciences).

Immunohistochemistry

Mice were sacrificed by overdose of pentobarbital and perfusion-fixed with 4% paraformaldehyde (Wako) at physiological perfusion pressure. Then, aortic specimens were dissected, rinsed with cold PBS and immediately frozen in OCT compound on a block of dry ice. Sections (10 μm) were cut from the specimens. The frozen sections were washed three times with 0.05% PBS-T then covered with anti-CD68 antibody (1:200; MCA 1957, Serotec), anti-MMP9 antibody (1:50; AF909, R&D), anti-MCP-1 antibody (1:50; ab25124, abcam) or anti-αSMA antibody (1:200; 1A4, Sigma-Aldrich), and incubated at 4°C overnight. The sections were washed three times with PBS-T and incubated with anti-rat secondary antibody for 30 minutes at room temperature. Then the sections were rinsed again three times with PBS-T, and covered with mounting medium with 4',6-diamidino-2-phenylindole (DAPI; H-1200, Vectashield). The positively stained areas of each aorta were measured using a digital fluorescence microscope (BZ-9000, Keyence).

Statistics

If the data were not obviously normally distributed, distributions of all variables were tested using the Shapiro–Wilk test. Equal variance between groups was tested by the F test. The non-parametric Mann-Whitney test was used to compare data that did not follow a normal distribution or equal variance. Accordingly, AAA type in the AngII model was compared with the Chi-square test for trend. Survival of AAA was compared using the log-rank test. One-way analysis of variance (ANOVA) followed by Tukey's multiple comparison test (or Dunn's multiple comparison test for non-parametric method) were used for one-factorial experiments. Two-way ANOVA followed by Tukey's or Bonferroni's multiple comparison test were used for two-factorial experiments. Results are expressed as mean ± standard error of the mean (SEM). A p-value < 0.05 was considered statistically significant. Statistical analyses were conducted using R 3.1.0 (R Foundation for Statistical Computing, Vienna, Austria) and Prism6 (GraphPad Software, Inc. USA).

Supplemental references

1. Horie T, Ono K, Nishi H, Nagao K, Kinoshita M, Watanabe S, Kuwabara Y, Nakashima Y, Takanabe-Mori R, Nishi E, Hasegawa K, Kita T, Kimura T. Acute doxorubicin cardiotoxicity is associated with miR-146a-induced inhibition of the neuregulin-ErbB pathway. *Cardiovasc Res*. 2010;87(4):656-664. doi:10.1093/cvr/cvq148.

2. Horie T, Baba O, Kuwabara Y, Chujo Y, Watanabe S, Kinoshita M, Horiguchi M, Nakamura T, Chonabayashi K, Hishizawa M, Hasegawa K, Kume N, Yokode M, Kita T, Kimura T, Ono K. MicroRNA-33 deficiency reduces the progression of

atherosclerotic plaque in ApoE-/- mice. *J Am Heart Assoc*. 2012;1(6):e003376. doi:10.1161/JAHA.112.003376.

3. Daugherty A, Manning MW, Cassis LA. Angiotensin II promotes atherosclerotic lesions and aneurysms in apolipoprotein E–deficient mice. *J Clin Invest*. 2000;105(11):1605-1612. doi:10.1172/JCI7818.

4. Longo GM, Xiong W, Greiner TC, Zhao Y, Fiotti N, Baxter BT. Matrix metalloproteinases 2 and 9 work in concert to produce aortic aneurysms. *J Clin Invest*. 2002;110(5):625-632. doi:10.1172/JCI15334.

5. Daugherty A, Manning MW, Cassis LA. Antagonism of AT2 receptors augments Angiotensin II-induced abdominal aortic aneurysms and atherosclerosis. *British Journal of Pharmacology*. 2001;134(4):865-870. doi:10.1038/sj.bjp.0704331.

6. Van Eck M, Singaraja RR, Ye D, Hildebrand RB, James ER, Hayden MR, Van Berkel TJC. Macrophage ATP-binding cassette transporter A1 overexpression inhibits atherosclerotic lesion progression in low-density lipoprotein receptor knockout mice. *Arterioscler Thromb Vasc Biol*. 2006;26(4):929-934. doi:10.1161/01.ATV.0000208364.22732.16.

7. Aparicio-Vergara M, Shiri-Sverdlov R, de Haan G, Hofker MH. Bone marrow transplantation in mice as a tool for studying the role of hematopoietic cells in metabolic and cardiovascular diseases. *Atherosclerosis*. 2010;213(2):335-344. doi:10.1016/j.atherosclerosis.2010.05.030.

8. Horie T, Nishino T, Baba O, Kuwabara Y, Nakao T, Nishiga M, Usami S, Izuhara M, Sowa N, Yahagi N, Shimano H, Matsumura S, Inoue K, Marusawa H, Nakamura T, Hasegawa K, Kume N, Yokode M, Kita T, Kimura T, Ono K. MicroRNA-33 regulates sterol regulatory element-binding protein 1 expression in mice. *Nat Comms*. 2013;4:2883. doi:10.1038/ncomms3883.

9. Palamakumbura AH, Trackman PC. A fluorometric assay for detection of lysyl oxidase enzyme activity in biological samples. *Anal Biochem*. 2002;300(2):245-251. doi:10.1006/abio.2001.5464.

10. Galis ZS, Sukhova GK, Libby P. Microscopic localization of active proteases by in situ zymography: detection of matrix metalloproteinase activity in vascular tissue. *The FASEB Journal*. 1995. doi:10.1096/fj.1530-6860.

11. Mook ORF, Van Overbeek C, Ackema EG, Van Maldegem F, Frederiks WM. In situ localization of gelatinolytic activity in the extracellular matrix of metastases of colon cancer in rat liver using quenched fluorogenic DQ-gelatin. *J Histochem Cytochem*. 2003;51(6):821-829.

12. Lund AK, Lucero J, Lucas S, Madden MC, McDonald JD, Seagrave JC, Knuckles TL, Campen MJ. Vehicular Emissions Induce Vascular MMP-9 Expression and Activity Associated With Endothelin-1-Mediated Pathways. *Arterioscler Thromb Vasc Biol*. 2009;29(4):511-517. doi:10.1161/ATVBAHA.108.176107.